2-1-2020

Essential Role for Integrin-Linked Kinase in Melanoblast Colonization of the Skin

Melissa Crawford
Children's Health Research Institute, London, ON

Valerie Leclerc
Children's Health Research Institute, London, ON

Kevin Barr
Children's Health Research Institute, London, ON

Lina Dagnino
Children's Health Research Institute, London, ON, ldagnino@uwo.ca

Essential Role for Integrin-Linked Kinase in Melanoblast Colonization of the Skin

Melissa Crawford[1], Valerie Leclerc[1], Kevin Barr[1] and Lina Dagnino[1,2]

Melanocytes are pigment-producing cells found in the skin and other tissues. Alterations in the melanocyte lineage give rise to a plethora of human diseases, from neurocristopathies and pigmentation disorders to melanoma. During embryogenesis, neural crest cell subsets give rise to two waves of melanoblasts, which migrate dorsolaterally, hone to the skin, and differentiate into melanocytes. However, the mechanisms that govern colonization of the skin by the first wave of melanoblasts are poorly understood. Here we report that targeted inactivation of the integrin-linked kinase gene in first wave melanoblasts causes defects in the ability of these cells to form long pseudopods, to migrate, and to proliferate in vivo. As a result, integrin-linked kinase–deficient melanoblasts fail to populate normally the developing epidermis and hair follicles. We also show that defects in motility and dendricity occur upon integrin-linked kinase gene inactivation in mature melanocytes, causing abnormalities in cell responses to the extracellular matrix substrates collagen I and laminin 332. Significantly, the ability to form long protrusions in mutant cells in response to collagen is restored in the presence of constitutively active Rac1, suggesting that an integrin-linked kinase-Rac1 nexus is likely implicated in melanocytic cell establishment, dendricity, and functions in the skin.

Journal of Investigative Dermatology (2020) **140,** 425–434; doi:10.1016/j.jid.2019.07.681

INTRODUCTION

The neural crest is a transient structure that forms in the dorsal region of the developing neuronal epithelium and is composed of multipotent cells. Neural crest cells undergo epithelial-mesenchymal transition soon after their formation during neural tube closure and begin to migrate to invade the developing embryo. These cells are essential for the generation of pigmented melanocytes and contribute to the cardiovascular and peripheral nervous systems (Le Douarin and Dupin, 2018). The behavior of neural crest cells is strongly influenced by interactions with their surrounding environment (Wang and Astrof, 2016). Integrins containing β1 or β3 subunits are particularly important for these interactions, as they modulate motility along the dorsolateral pathway and survival of neural crest cells and their progeny (Testaz and Duband, 2001). Additionally, β1 integrins are required for the normal establishment of the melanocyte lineage (Moore and Larue, 2004).

Melanoblasts are generated from neural crest cells that embark on two distinct migration waves during development. The first wave involves a subset of neural crest cells that delaminate from the neural tube at embryonic day (E) 9 in mice. Around E10.5, some neural crest cells give rise to melanoblasts, which express *Mitf, Dct,* and *Pmel17* (Baxter and Pavan, 2003). Melanoblasts spread from areas adjacent to the neural tube along a dorsolateral path toward the developing dermis. The second wave occurs around E14.5 when Schwann cell precursors, generated from neural crest cells that moved along the ventral pathway associating with nerve endings, subsequently differentiate into melanoblasts (Adameyko et al., 2009; Colombo et al., 2012; Mort et al., 2015). By E15.5, all melanoblasts localize to the basal layer of the epidermis, and by E16.5 they have also populated the developing hair follicles (Adameyko et al., 2009), later giving rise to mature melanocytes and melanocyte stem cells.

Integrin-linked kinase (ILK) is an important cytoplasmic effector of β1 integrins and, as such, is a key transducer of cell interactions with the surrounding environment. ILK is necessary for cell polarization and embryo survival (Sakai et al., 2003), and its importance for actin cytoskeletal dynamics, as well as integrin modulation of cell adhesion and migration, has been clearly established in metazoans. For example, ILK-containing complexes transduce signals that inhibit integrin endocytic turnover at the plasma membrane, thus reinforcing integrin-extracellular matrix (ECM) adhesion in Drosophila embryos (Vakaloglou et al., 2016). In mouse epidermis, ILK is essential for hair follicle morphogenesis, epidermal integrity and barrier function, as well as keratinocyte polarization, directional migration, and survival (Im and Dagnino, 2018; Nakrieko et al., 2008; Sayedyahossein et al., 2016). *Ilk* inactivation in E8.5 neural crest cell subsets that contribute to cardiac outflow tract formation results in defective focal adhesion formation and severe cardiac defects (Dai et al., 2013). Given the importance of ILK in ectodermal and neural crest cell–derived tissues, we have investigated its role in the establishment and characteristics of melanocytic cells in the skin. We now show that ILK plays

[1]*Department of Physiology and Pharmacology, Children's Health Research Institute, Lawson Health Research Institute, London, Ontario, Canada; and* [2]*Department of Oncology, University of Western Ontario, London, Ontario, Canada*

Correspondence: Lina Dagnino, Department of Physiology and Pharmacology, Medical Sciences Building, University of Western Ontario, London, Ontario N6A 5C1, Canada. E-mail: ldagnino@uwo.ca

Abbreviations: E, embryonic day; ECM, extracellular matrix; GFP, green fluorescent protein; ILK, integrin-linked kinase; KO, knockout; 4-OHT, 4-hydroxytamoxifen

Received 29 January 2019; revised 21 June 2019; accepted 2 July 2019; accepted manuscript published online 19 July 2019; corrected proof published online 26 September 2019

key roles in first wave embryonic melanoblast trafficking and melanocyte interactions with the ECM, and that ILK is essential for melanocytic cell colonization of the skin.

RESULTS

Defects in melanoblast ability to populate the skin in the absence of ILK

To investigate the role of ILK in the first wave of melanogenesis, we developed a reporter mouse model in which Cre-mediated coordinate inactivation of loxP-flanked *Ilk* alleles and expression of membrane-targeted green fluorescent protein (GFP) are induced specifically in melanocytic lineage cells upon administration of tamoxifen at E11.5. In these animals, non-targeted cells express a membrane-bound form of Tomato fluorescent protein. Analysis of skin sections generated from E20.5 embryos that were heterozygous for the loxP-flanked *Ilk* allele (*Tyr::CreER^{T2}*, *ROSA$^{mT/mG}$*, *Ilk$^{f/+}$*, hereafter termed ILK^{+}), and which were exposed to tamoxifen at E11.5, revealed subsets of cells that expressed GFP in some hair follicles and in the interfollicular epidermis. These GFP^{+} cells also expressed the melanocyte-specific enzyme marker dopachrome-tautomerase, confirming their melanocytic identity (Supplementary Figure S1 and data not shown). Similarly, GFP^{+} cells were detected in hair follicles from *Ilk$^{f/f}$* homozygous *Tyr::CreER^{T2}*, *ROSA$^{mT/mG}$*, *Ilk$^{f/f}$* (hereafter termed ILK knockout [ILK^{KO}]) mice (Supplementary Figure S1).

We next analyzed the consequences of *Ilk* gene inactivation on cutaneous embryonic melanocytic cell abundance. Truncal melanoblasts are scarce, and about 18,000 cells have been estimated to exist in each E15.5 embryo, mainly localized to the epidermis and the developing hair follicle (Delmas et al., 2007). Given that our tamoxifen treatments were designed to target only the first wave of melanoblasts and given the potential intrinsic efficiency limitations of tamoxifen-inducible Cre recombination in vivo, we generated single-cell suspensions from the skin of E15.5 ILK^{+} and ILK^{KO} embryos that had been treated with tamoxifen at E11.5. We subsequently analyzed the proportion of GFP^{+} melanoblasts in these isolates by flow cytometry. The number of GFP-positive ILK^{+} melanoblasts per embryo ranged from 50 to 1,400, averaging ~470 (n = 14 embryos), and constituting ~0.1% of the entire skin cell population isolated, and ~3% of the estimated total number of melanoblasts in E15.5 skin (Delmas et al., 2007). Inactivation of *Ilk* resulted in a ~60% reduction in the number of cutaneous trunk ILK^{KO} melanoblasts, which averaged ~200 cells/embryo (Figure 1a). There was negligible non-induced Cre activity, with only 0.002% of GFP^{+} cells (~10 cells/embryo) detected in isolates from embryos that had not received tamoxifen (Figure 1a). Analysis of tissue sections from E17.5 embryos also revealed a deficit of ILK^{KO} melanocytic cells. Specifically, we detected a ~50% reduction in GFP^{+} ILK^{KO} cells located in the interfollicular epidermis, relative to ILK^{+} cells. Similar proportions of developing hair follicles exhibiting GFP^{+} melanoblasts were observed in ILK^{+} and ILK^{KO} animals (Figure 1b). Notably, in E20.5 embryos, the mean number of GFP-positive ILK^{+} and ILK^{KO} melanoblasts per 6 mm of interfollicular epidermis was, respectively, 18 and 1, indicating a ~96% reduction in the abundance of ILK-deficient melanoblasts, relative to ILK-expressing cells (Figure 1c). At this time, there was also a ~4-fold decrease in the proportion of hair follicles with detectable GFP^{+} melanocytic cells in ILK^{KO} tissues, relative to those expressing ILK (Figure 1c). Together, these observations indicate that ILK is essential for the normal establishment of cutaneous melanoblast populations in vivo. To determine if these alterations caused postnatal pigmentation defects, E20.5 embryos were delivered by cesarean section, because the tamoxifen treatment interfered with parturition. The coat color patterns in ILK^{KO} mice were indistinguishable from those of ILK^{+} animals as late as 3 weeks of age (data not shown), likely because of the presence of a significant fraction of untargeted melanocytes in the hair follicles.

Abnormal motility and proliferation of embryonic ILK^{KO} melanoblasts

Complex interactions between embryonic melanoblasts and their surrounding environment determine their ability to migrate through various tissues, home to the skin, and eventually distribute throughout the epidermis and the hair follicles (Petit and Larue, 2016). Given the decreased abundance of ILK^{KO} melanoblasts as early as E15.5, we next determined if these cells exhibit defective motility. To this end, we first developed a system that supports culture of embryonic melanoblasts for subsequent analyses. We isolated single-cell suspensions of cutaneous cells from ILK^{+} and ILK^{KO} E15.5 embryos that had been exposed to tamoxifen at E11.5. GFP^{+} melanoblasts were then purified by FACS. In these isolates, we first evaluated the proportion of GFP^{+} viable cells, defined as the population that was negative for both 7-aminoactinomycin D- and Annexin V-associated fluorescence. We found that in each isolate, ≥85% of cells were viable (Supplementary Figure S2a). These FACS-purified cells were then seeded on ST2 bone marrow–derived mesenchymal stem cell-like feeder layers. Under these conditions, melanoblasts remained viable for at least a week, the longest interval after isolation we tested. Further, all GFP^{+} melanoblasts were able to transition into TYRP1-expressing, melanin-producing cells by day 7 after isolation, and no longer exhibited detectable membrane-bound Tomato protein–associated fluorescence, irrespective of whether or not they expressed ILK (Supplementary Figure S2b), although the abundance of ILK^{KO} melanoblasts was lower than that of ILK^{+} cells by this time (data not shown).

Melanoblast migration through embryonic tissues is modulated through attractive and repulsive interactions with the ECM and with adjacent cells. In particular, ECM proteins, such as laminins and collagen, provide adhesive substrates that melanoblasts can use for integrin-mediated attachment and directional movement (Laurent-Gengoux et al., 2018; Petit and Larue, 2016). Thus, we first investigated if ILK is necessary for proper melanoblast adhesion. Although both ILK-expressing and ILK-deficient melanoblasts had attached to the ST2 feeder layers 16 hours after FACS-purification and plating, there were clear morphologic differences between the two melanoblast types. Specifically, whereas ~70% of ILK^{+} melanoblasts displayed a well-spread morphology and exhibited multiple protrusions, ~77% of ILK^{KO} cells failed to spread, as evidenced by their spherical morphology

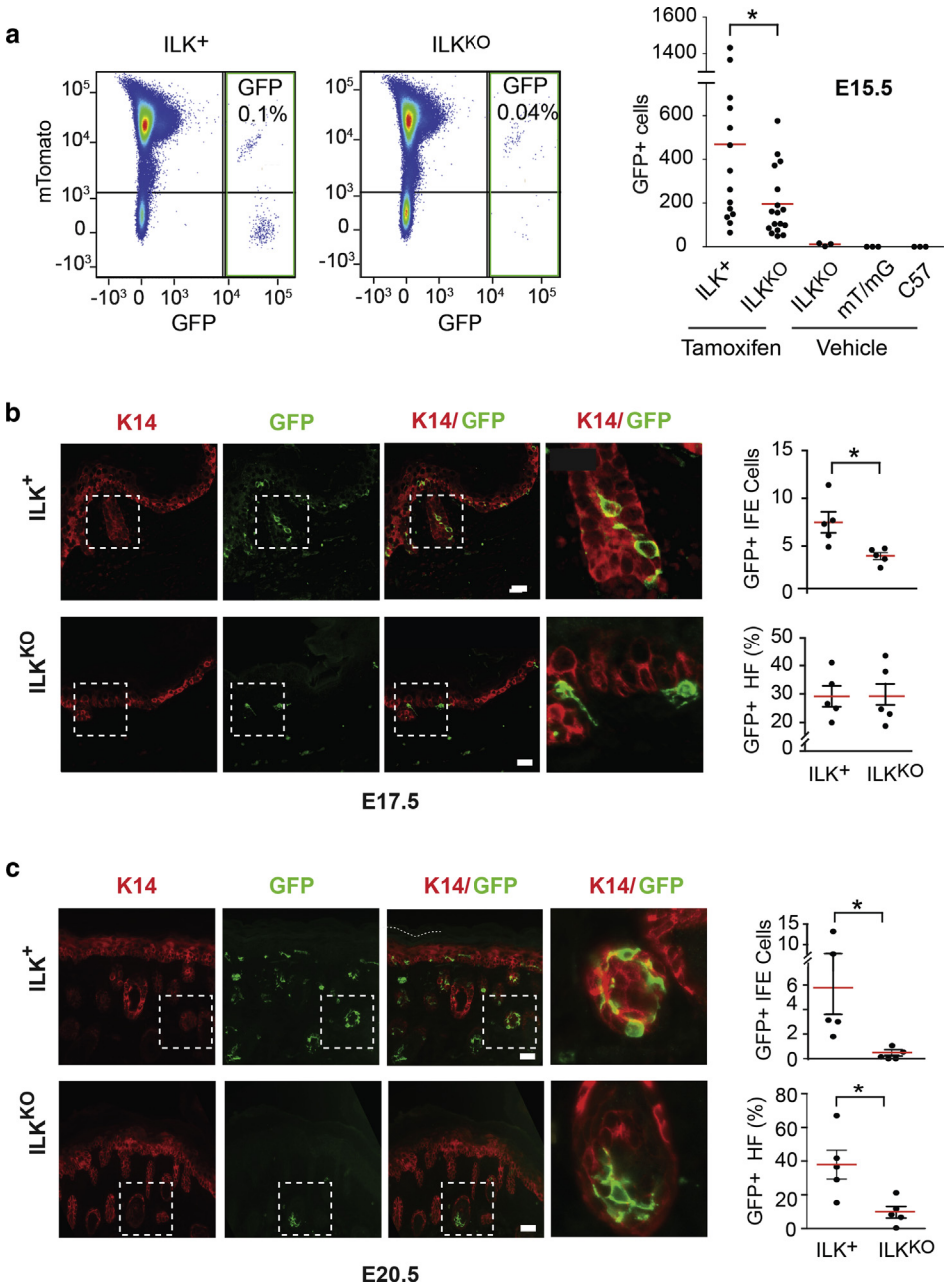

Figure 1. Defects in ILK-deficient embryonic melanoblast populating the skin. (**a**) FACS dot plots of dissociated skin cells from ILK^{+} and ILK^{KO} E15.5 littermate embryos analyzed according to mTomato and GFP fluorescence intensities. The associated graph shows the number of viable (i.e., 7-AAD-negative) GFP-positive cells in individual embryos obtained from 4–5 independent litters of tamoxifen-treated ILK^{+} and ILK^{KO} mice, or 1 litter for embryos treated with vehicle. Red lines represent the mean number of GFP-positive cells in each group. mTmG and C57 indicate *Ilk$^{f/f}$; mT/mG,* and C57BL/6J mice, respectively. *$P < 0.05$, Student *t* test. (**b, c**) Skin sections from embryos of the indicated gestational ages were processed for IF microscopy with antibodies against K14 or GFP. Insets are shown at higher magnification in the adjacent micrographs.. The graphs represent the mean ± SEM of GFP-positive melanocytic cells per 2 mm of IFE, or the mean percentage ± SEM of HF containing GFP-positive melanocytes. Plots show results from five different embryos of each genotype (three independent litters). *$P < 0.05$, Student *t* test. 7-AAD, 7-Aminoactinomycin D; E, embryonic day; GFP, green fluorescent protein; HF, hair follicles; IF, immunofluorescence; IFE, interfollicular epidermis; ILK, integrin-linked kinase; K14, keratin 14; KO, knockout; mTomato, membrane-bound Tomato fluorescent protein; 4-OHT, 4-hydroxytamoxifen; SEM, standard error of the mean. Bar= 25 μm

(Figure 2a and b). Time-lapse videomicroscopy analysis of well-spread melanoblasts of both genotypes revealed highly dynamic extension and retraction of pseudopods. The formation of long pseudopods is a requirement for optimal migration and homing of embryonic melanoblasts. Hence, we assessed the ability of these cells to generate long protrusions, ≥20 μm in length, during a 3-hour recording period. Whereas 55% of ILK^{+} cells generated at least one long protrusion, only 16% of spread ILK^{KO} melanoblasts did (Figure 2b). Random motility of well-spread ILK^{+} and ILK^{KO} cells 1–3 days after initial seeding recorded over 3-hour intervals was similar, with ~60% of these cells migrating ≤50 μm (Figure 2c and d). In contrast, ~50% of non-spread ILK^{KO} melanoblasts exhibited total migration distances >100 μm, with proportionally higher velocities (Figure 2c and d). Significantly, the mean directional persistence of cell movement ("Directionality", calculated as Euclidean divided by total distance migrated) was significantly greater in ILK^{+} cells (0.46) than in either spread or non-spread ILK^{KO} cells (0.32 and 0.17, respectively; Figure 2e). Thus, ILK is essential for normal spreading, pseudopod formation, and persistence of directional motility in embryonic melanoblasts.

We also determined if *Ilk* inactivation alters melanoblast proliferation or apoptosis, which might contribute to the reduced abundance of cutaneous E15.5 ILK^{KO} melanoblasts. Pregnant dams treated with tamoxifen at 11.5 days of gestation subsequently received 5-ethynyl-2′-deoxyuridine 3 hours before embryo harvesting; melanoblasts were FACS-purified, plated on ST2 feeder layers, allowed to attach, and processed for microscopy 16 hours later. This approach

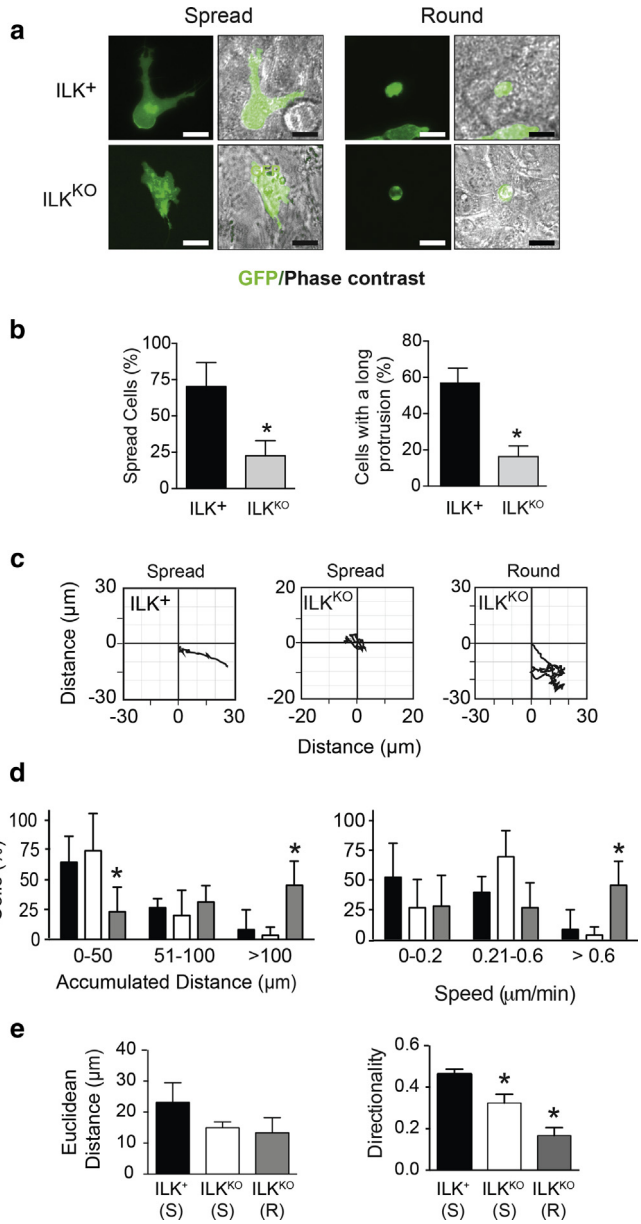

Figure 2. Impaired spreading and motility in ILK^{KO} melanoblasts. GFP-expressing melanoblasts from E15.5 tamoxifen-treated mouse embryos of the indicated genotype were isolated by FACS and seeded on ST2 cell feeder layers. (**a**) GFP IF and GFP and phase-contrast overlay micrographs of melanoblasts 1 day after seeding. (**b**) The mean percentage of cells (and SD) that exhibited spread morphology after 1 day in culture and those cells that generated at least one pseudopodium >20 μm in length during a 3-hour time-lapse videorecording period during the first 3 days of culture are indicated in the histograms. For each genotype, >60 melanoblasts isolated from four different litters were scored. *$P < 0.05$, Student t test. **(c–e)** S or R melanoblasts were recorded by time-lapse videomicroscopy in 3-hour intervals, over 3 days of culture. Single-cell plots for random migration tracks were obtained (panel c), from which accumulated distance, speed, Euclidean distance, and directionality were calculated and are presented as mean ± SD (panels d and e). In the histograms of panels d and e, the data for spread ILK^{+} (black bars), spread ILK^{KO} (white bars), and round ILK^{KO} cells (gray bars) are shown. *$P < 0.05$, ANOVA (40 cells scored from four independent isolates). ANOVA, analysis of variance; E, embryonic day; GFP, green fluorescent protein; IF, immunofluorescence; ILK, integrin-linked kinase; KO, knockout; R, round; S, spread; SD, standard deviation. Bar= 25 μm.

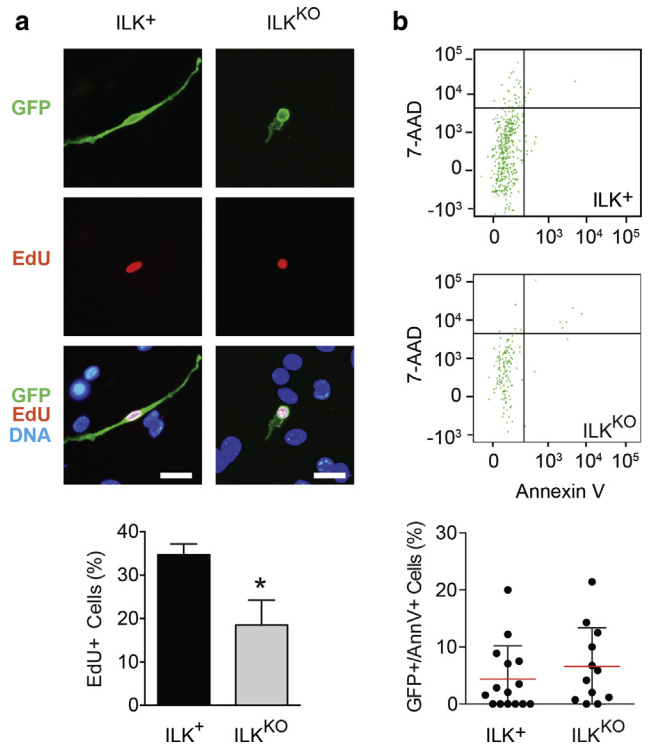

Figure 3. Impaired proliferative capacity in ILK^{KO} melanoblasts. (**a**) Representative micrographs of GFP-expressing melanoblasts isolated from embryos of the indicated genotype treated with tamoxifen and EdU, and seeded onto ST2 feeder layers. The cells were processed for IF microscopy 16 hours after seeding to detect EdU, and also using anti-GFP antibodies. DNA was visualized with Hoechst 33342. The histogram represents the mean percentage ± SD of EdU^{+} melanoblasts (360 cells from three independent isolates obtained from 14 ILK^{+} embryos; 70 cells from three independent isolates obtained from 24 ILK^{KO} embryos). *$P < 0.05$, Student t test. **(b)** Representative flow cytometry plots of melanoblast cell suspensions incubated with 7-AAD and AnnV. The graph represents the percentage of AnnV- and GFP-positive melanoblasts in each of 12–15 embryos from three independent litters. Scale bars indicate mean ± SD. 7-AAD, 7-Aminoactinomycin D; AnnV, annexin V; EdU, 5-ethynyl-2′-deoxyuridine; GFP, green fluorescent protein; IF, immunofluorescence; ILK, integrin-linked kinase; KO, knockout; SD, standard deviation. Bar = 25 μm.

was necessary to simultaneously detect GFP immunoreactivity and 5-ethynyl-2′-deoxyuridine in this cell population. We found that ~35% and ~19% of ILK^{+} and ILK^{KO} melanoblasts, respectively, were 5-ethynyl-2′-deoxyuridine-positive, indicating an almost 2-fold reduction in the proportion of proliferative melanoblasts in the absence of ILK (Figure 3a). In addition, only ~4% of ILK^{+} melanoblasts were Annexin V-positive at isolation, a fraction that was indistinguishable from that observed in ILK^{KO} cells (Figure 3b). Collectively, these observations are consistent with the notion that deficits in embryonic ILK^{KO} melanoblast ability to populate the skin are likely owing, at least in part, to impaired proliferation, motility, and ability to interact with the extracellular milieu.

Abnormal proliferation and motility in postnatal ILK-deficient melanocytes

To better understand how *Ilk* inactivation affects postnatal melanocytic cell functions, we characterized primary

melanocytes isolated from 3-day-old mice and cultured to ≥95% purity. Cre-mediated excision of the loxP-containing *Ilk* alleles was exclusively observed in cultures treated with 4-hydroxytamoxifen (4-OHT), although only ∼50% of the cells appeared to be targeted, as indicated by the fraction of GFP-expressing cells in the cultures (Supplementary Figure S3). ILK protein levels in FACS-purified GFP^+ melanocytes 5 days after treatment with 4-OHT were barely detectable and were similar to those in lysates prepared from cells that had been incubated with a Cre-encoding adenovirus with >90% transduction efficiency (Supplementary Figure S3). Membrane-bound Tomato protein fluorescence was detectable in all melanocytes as late as 5 days after the initial 4-OHT treatment. We also measured the proliferation and apoptosis status in the cultures and found Ki67 immunoreactivity in ∼40% of ILK-expressing and ∼18% of ILK-deficient melanocytes (Figure 4a). Negligible fractions of melanocytes showed either fragmented nuclear DNA or caspase 3/7 activity, irrespective of the presence or absence of ILK (Figure 4b and c). Thus, the proliferative defects observed in ILK^{KO} melanoblasts were maintained in ILK-deficient postnatal melanocytes.

Epidermal melanocytes interact in vivo with laminin 332 present in the basement membrane (Haass et al., 2005). In culture, laminin 332 promotes motility in primary melanocytes (Crawford et al., 2017). Therefore, we next examined the role of ILK in melanocyte migration, recording single melanocytes for 16 hours using time-lapse videomicroscopy. Cell trajectory plot analyses revealed that 43% of ILK-expressing and only 2% of GFP^+ ILK-deficient melanocytes migrated distances >300 μm. During this time interval, ILK-expressing and ILK-deficient cells moved on average ∼307 μm and ∼87 μm, respectively, which was reflected in a ∼3.5-fold difference in speed (Figure 5). Thus, ILK is required to maintain normal postnatal melanocyte proliferation and for random migration on laminin-332 substrates.

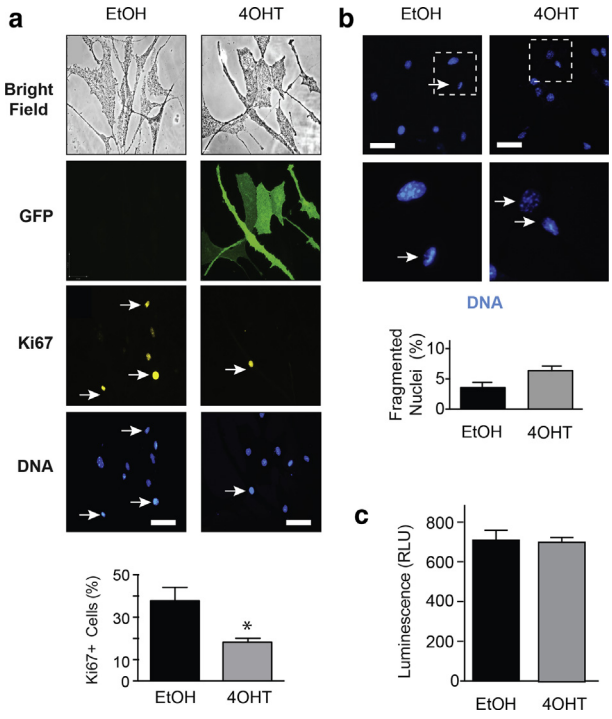

Figure 4. Proliferation defects in ILK-deficient melanocytes. Epidermal melanocytes were isolated from 3-day-old *TyrCreERT2, mT/mG, Ilk$^{f/f}$* mice and cultured to passage 2−3. Cells were treated with 1 μM 4-OHT or control vehicle (0.25% EtOH) for 48 hours, and cultured for an additional 72-hour interval. (**a**) Cells were processed for IF microscopy using anti-GFP and anti-Ki67 antibodies. DNA was visualized with Hoechst 333412. The corresponding phase-contrast micrographs are also shown. The arrows indicate examples of GFP- and Ki67-positive cells. (**b**) Melanocyte nuclei were scored for the presence of condensed and/or fragmented DNA after staining with Hoechst 33342, indicated by arrows. (**c**) Melanocyte lysates were prepared 120 hours after treatment with EtOH or 4-OHT. Relative caspase 3/7 activities were determined using a proluciferin caspase substrate in the presence of luciferase, as described in the Materials and Methods, and measuring luminescence in RLU. The histograms indicate the mean ± SEM, with only GFP-positive cells scored in the 4-OHT group in panels a and b. *$P < 0.05$, Student *t* test (n = 3). EtOH, ethanol; GFP, green fluorescent protein; IF, immunofluorescence; ILK, integrin-linked kinase; 4-OHT, 4-hydroxytamoxifen; RLU, relative light units; SEM, standard error of the mean. Bar= 50 μm.

Modulation of melanocyte dendricity by ILK

Laminin 332 and collagens promote dendrite formation in melanocytes (Crawford et al., 2017; Hara et al., 1994). Dendritic extensions are essential for melanocyte interactions with the epidermal basement membrane and with neighboring keratinocytes. We found that ∼80% of ILK-expressing melanocytes seeded on laminin 332 matrix generated on average 3−4 dendrites per cell, with at least one dendrite measuring ≥14 μm in length (Supplementary Figure S4). Inactivation of *Ilk* resulted in a 25% reduction in the fraction of dendritic melanocytes, which generated on average only approximately two dendrites per cell (Supplementary Figure S4).

We also analyzed the role of ILK on melanocyte morphologic changes in response to Mn^{2+}. This cation promotes formation of dendrites in primary human melanocytes (Hara et al., 1994) and can induce conformational changes in integrins, such that their on-rates of binding to ligands are increased (Mould et al., 2002). Cells were suspended in growth medium supplemented with 0.1 mM $MnCl_2$ and seeded onto a laminin 332 matrix. We then assessed time-dependent decreases in circularity (a ratio of cell surface area to perimeter), as a measure indicative of melanocyte spreading and dendricity (Robinson et al., 2019). Mn^{2+} significantly accelerated the formation of cell extensions within the first 30 minutes after seeding in ILK-expressing melanocytes, as evidenced by a decrease in mean circularity values from 0.71 to 0.62 in the absence and presence of this ion, respectively (Supplementary Figure S5a). Circularity values in these cells further decreased after 60 minutes but were no longer affected by the presence of Mn^{2+}. In stark contrast, circularity values in ILK-deficient cells were not altered by Mn^{2+}, and were significantly higher than those in normal melanocytes at all times analyzed (Supplementary Figure S5a). Significantly, both ILK-expressing and ILK-deficient cells seeded in the absence of exogenous ECM substrates exhibited circularity values in the 0.80 range, irrespective of whether or not Mn^{2+} was present (Supplementary Figure S5b). Similar experiments were conducted with cells suspended in medium with or without Mn^{2+}, but plated on collagen I. Because the development of pseudopodal extensions in melanocytes seeded on collagen required longer intervals and was less pronounced than in cells plated on laminin 332 matrix,

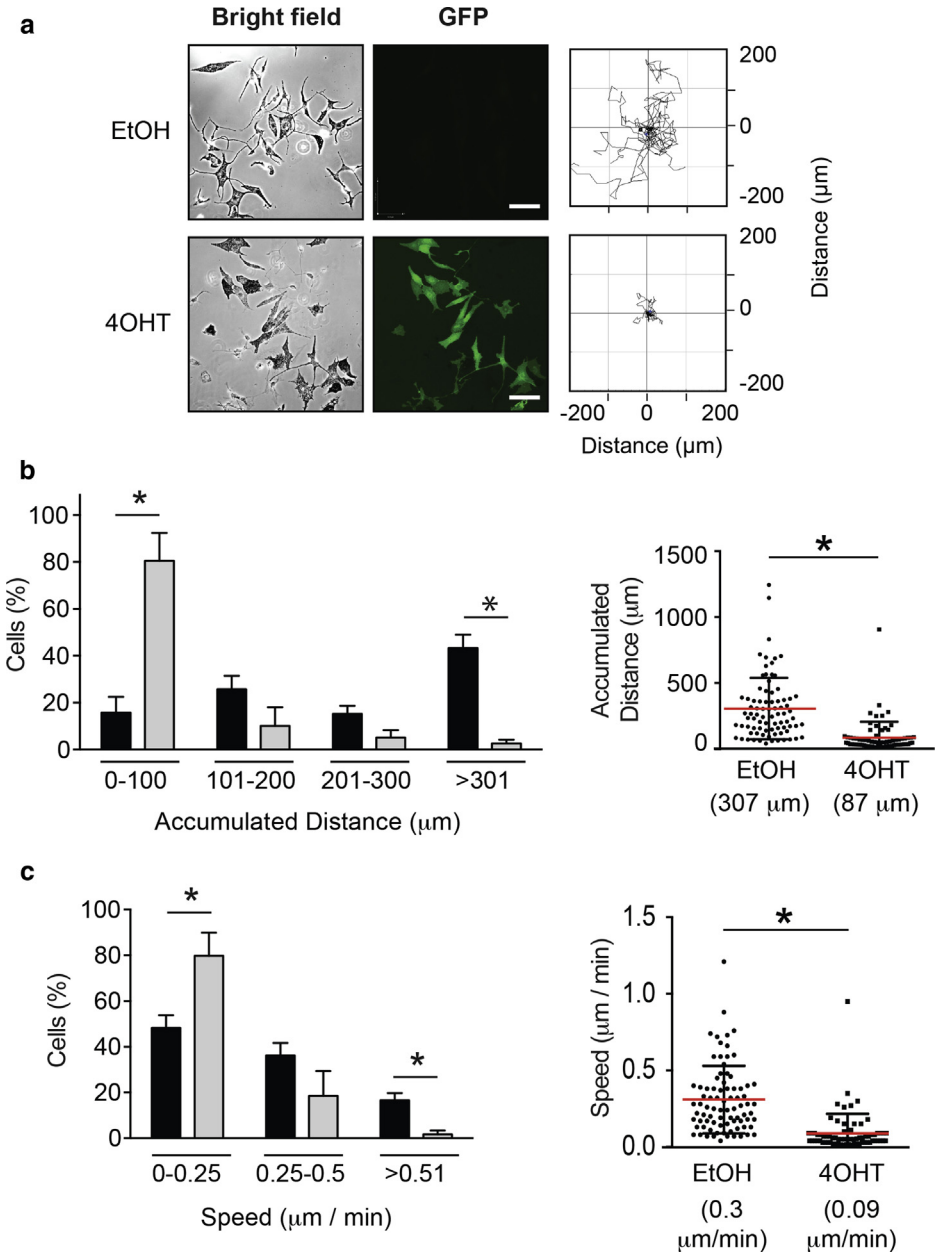

Figure 5. Motility defects in ILK-deficient melanocytes. Epidermal melanocytes were isolated from 3-day-old *TyrCreERT2, mT/mG, Ilk*$^{f/f}$ mice and cultured to passage 2−3. Cells were treated with 1 μM 4-OHT or control vehicle (0.25% EtOH) for 48 hours, and cultured for an additional 72-hour interval. (**a**) Representative phase-contrast and GFP-fluorescence micrographs of cells that were recorded by time-lapse videomicroscopy for 16 hours. The adjacent diagrams show cell trajectory plots. (**b, c**) The percentage of ILK-expressing melanocytes (black bars) and ILK-deficient and/or GFP-positive cells (gray bars) that traveled the accumulated distance (panel b) and speed (panel c) ranges shown were calculated. The histograms show the mean ± SD. Numbers in brackets indicate the average distance or speed. *$P < 0.05$, Student *t* test (70−95 cells scored from four independent isolates). EtOH, ethanol; GFP, green fluorescent protein; ILK, integrin-linked kinase; 4-OHT, 4-hydroxytamoxifen; SD, standard deviation. Bar= 70 μm.

we measured cell surface area, rather than circularity, 2 hours after seeding. The presence of Mn^{2+} increased surface area in both types of melanocytes. However, the loss of ILK was associated with attenuated responses to collagen, as evidenced by the ∼40% lesser mean surface area values measured in ILK-deficient cells (Supplementary Figure S5c). Together, our results suggest that the effects observed in cells seeded on laminin 332 matrix or collagen I may be associated with integrin activation and indicate that ILK is necessary to transduce signals from those ECM substrates, ultimately promoting spreading and formation of cell extensions.

Role of ILK in Rac1 activation

In melanocytes, paracrine basic fibroblast growth factor and other growth factors promote dendricity, through mechanisms that involve activation of Rac1 (Scott and Leopardi, 2003; Shi et al., 2016). To investigate the role of ILK in this process, we cultured melanocytes without exogenous ECM substrates, but with growth medium supplemented with soluble factors that promote melanin synthesis and dendrite formation ("MD medium"). Under these conditions, the fraction of ILK-expressing cells that exhibited branched dendrites increased ∼30-fold relative to the normal ("basal") culture medium (from ∼2% to ∼60%; Supplementary Figure S6). In contrast, only a partial response was observed in GFP^{+} ILK-deficient melanocytes, in which ∼18% of cells showed branched dendrites, whereas >50% of these cells remained non-dendritic (Supplementary Figure S6).

ILK contributes to Rac1 activation in response to growth factors and ECM substrates in various cell types (Ho and Dagnino, 2012; Lorenz et al., 2007; Sayedyahossein et al., 2012). Similarly, treatment of melanocytes with basic

fibroblast growth factor induces Rac1 activation and motility (Shi et al., 2016). Hence, we next investigated if ILK is involved in Rac1 activation in melanocytes. Analysis of FACS-purified GFP$^+$, ILK-deficient cells generated by 4-OHT treatment revealed no significant decreases in Rac1 protein levels, relative to ILK-expressing melanocytes (Supplementary Figure S7a). Because Rac1 activity assays were not possible using FACS-purified GFP$^+$ ILK-deficient melanocytes, we measured changes in active Rac1-GTP levels in cultures pretreated with 4-OHT and subsequently incubated for 16 hours in the absence of growth supplements, followed by stimulation with culture medium containing basic fibroblast growth factor. In these cultures, we estimated that *Ilk* gene inactivation occurred in ~40% of the melanocytes, based on the observed decrease in ILK abundance, without any significant changes in total Rac1 protein levels (Supplemental Figure S7b). Active Rac1-GTP levels increased ~2.5-fold 5 minutes after growth factor addition in control ILK-expressing cultures and returned to pre-stimulation levels by 10 minutes (Supplementary Figure S7c). In contrast, Rac1-GTP levels did not significantly change in response to basic fibroblast growth factor in 4-OHT-treated cultures, suggesting that at least some pathways involved in Rac1 activation are impaired in the absence of ILK.

In response to collagen I, melanocytes form cell protrusions in a Rac1-dependent manner (Crawford et al., 2017; Li et al., 2011). Thus, we next determined the relationship between ILK and Rac1-associated morphologic responses to this ECM substrate. To this end, we compared the ability of exogenously expressed Rac1 proteins to modulate melanocyte circularity, as a measure indicative of dendricity (Robinson et al., 2019). Sixteen hours after being seeded on collagen I, 56% of ILK-expressing melanocytes exhibited circularity values ≤0.13 (Figure 6). This fraction was not significantly altered by exogenous expression of wild type or constitutively active G12V Rac1. However, expression of dominant-negative T17N Rac1 decreased this proportion to ~25% (Figure 6d). In analogous experiments, we observed that only 29% of ILK-deficient cells exhibited circularity values ≤0.15, and this fraction was not altered by expression of either wild type or T17N Rac1. In contrast, expression of G12V Rac1 increased the proportion of ILK-deficient cells with circularity values ≤0.13 to 60%, which were indistinguishable from those in ILK-expressing cells (Figure 6c). Collectively, our findings suggest that ILK is necessary for transduction of signals from the ECM and/or growth factors that result in Rac1 activation and dendrite formation.

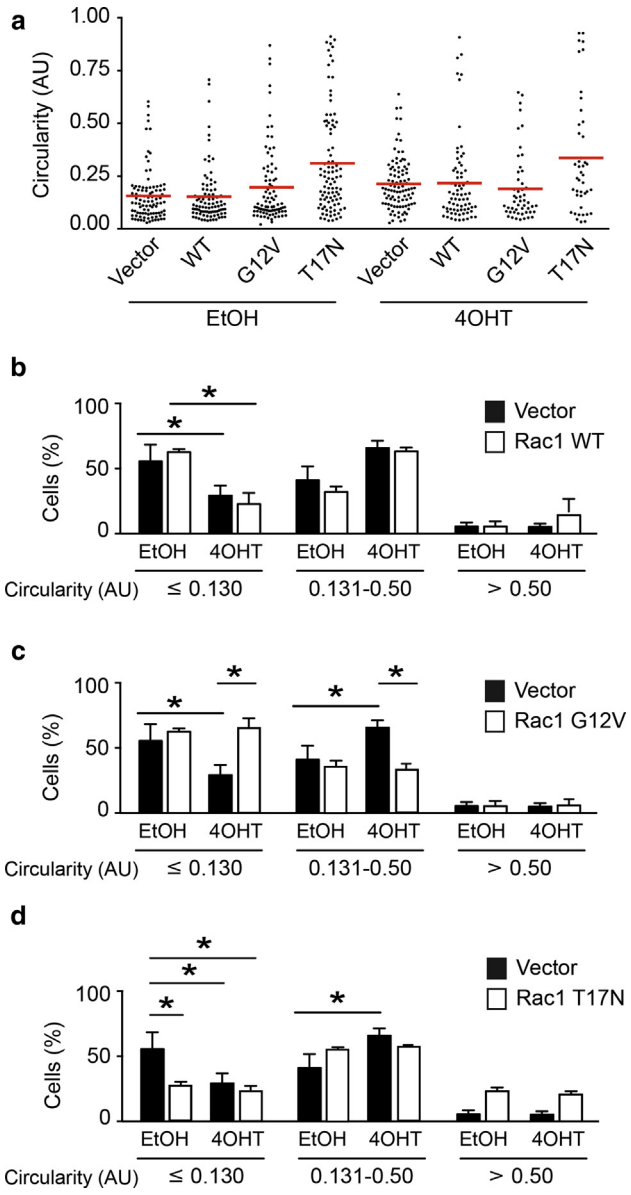

Figure 6. Expression of constitutively active Rac1 restores dendricity in ILK-deficient melanocytes. Epidermal melanocytes (passage 2–3) were isolated from 3-day-old *TyrCreERT2, mT/mG, Ilk$^{f/f}$* mice, and cultured for 48 hours with control vehicle (0.25% EtOH) or with 4-OHT to induce *Ilk* gene inactivation. Twenty-four hours after initial addition of 4-OHT, the cells were transfected with vectors encoding mCardinal ("Vector"), or mCardinal- and V5-tagged WT, constitutively active G12V, or dominant-negative T17N Rac1. Cells were cultured for an additional 48-hour period and were processed for IF microscopy. (**a**) Dot plots showing circularity values of individual ILK-expressing (EtOH) and ILK-deficient (4-OHT) melanocytes expressing the indicated Rac1 proteins. Horizontal bars show the mean values. (**b**–**d**) The percentage of EtOH- or 4-OHT-treated melanocytes transfected with empty vector (black bars) or the indicated Rac1 proteins (white bars), and with circularity values in the indicated ranges are expressed as the mean ± SEM. Only GFP$^+$ cells were scored in the 4-OHT treatment group. *$P < 0.05$, ANOVA (50–110 cells scored per group in three separate experiments using independent isolates). ANOVA, analysis of variance; EtOH, ethanol; GFP, green fluorescent protein; IF, immunofluorescence; ILK, integrin-linked kinase; 4-OHT, 4-hydroxytamoxifen; SEM, standard error of the mean; WT, wild type.

DISCUSSION

In this study, we report two major findings. First, we have established ILK as a previously unrecognized key contributor to processes that drive embryonic melanoblasts to populate the skin. Second, we show that melanocytes require activation of ILK-dependent pathways for normal interactions with the ECM, which, in turn, modulate motility and dendricity.

The reporter mouse model we generated allowed us to trace melanoblasts derived from neural crest cells during the

first wave of dorsolaterally migrating melanocytic cells. In this model, tamoxifen-induced *Ilk* gene inactivation occurred at E11.5, corresponding to a stage of active melanoblast proliferation and migration through the embryo (Luciani et al., 2011; Woodham et al., 2017). Although ILK-deficient melanoblasts were present in the E15.5 skin, their numbers were substantially reduced, likely because of abnormal proliferation and motility, rather than decreased viability at this stage. However, by E20.5, they were virtually undetectable in the interfollicular epidermis. In mice, melanocytic cells are present in the interfollicular epidermis as late as the perinatal period, and are subsequently found only in hair follicles. Given the defects in motility we observed in E15.5 melanoblasts and early postnatal melanocytes, it appears unlikely that the loss of interfollicular epidermal melanocytic cells we observed at E20.5 is because of migration out of this compartment. Whether this loss is associated with reduced viability remains an important area for future research. Our mouse model clearly established the importance of ILK in melanoblast colonization of the skin. However, our model did not allow us to determine the importance of ILK to overall hair pigmentation. Multiple factors likely contributed to the lack of obvious alterations in coat color. First, based on our analysis of ILK- and GFP-expressing embryonic melanoblasts, we estimate that only ~3% of all melanoblasts present at E15.5 are targeted in our mice, partly because tamoxifen did not likely target all first wave melanoblasts. Further, as many as 65% of melanocytes in postnatal hair follicles have been estimated to arise from Schwann precursors that give rise to the second wave of melanogenesis (Adameyko et al., 2009). In our model, melanocytic cells formed from Schwann cell precursors are not likely targeted because these cells are only born several days after tamoxifen administration. Indeed, in every hair follicle that contained GFP^+, ILK-deficient melanoblasts, we also observed a substantial presence of non-targeted melanocytes, which conceivably contribute to hair pigmentation. Pigmentation defects reported in genetically modified mouse models have been associated with as much as ~85% melanocyte depletion (Tokuo et al., 2018), well above the fraction of targeted melanocytes in our model.

The ST2-feeder-layer culture system we developed supported E15.5 skin melanoblast viability and differentiation into TYRP1-expressing, melanin-producing cells after 7 days in culture. This differs from the reported behavior of cKit-positive and/or CD45-negative putative melanoblasts isolated from E12.5 or E14.5 mouse skin, which generated multiple lineages when cultured on ST2 feeder layers, with only a minor proportion of melanin-producing cells (Watanabe et al., 2016). Whether our GFP^+ melanoblasts constitute a lineage-restricted fraction of the cKit-positive and/or CD45-negative population, or whether the culture conditions we used mimic embryonic skin environmental signals that instruct melanoblasts to evolve into melanin-producing cells is an important topic for future study.

Melanoblast expansion and homing to the skin during development are influenced by the surrounding environment and by genetic context. Our studies indicate impaired ability of ILK^{KO} melanoblasts to interact with their environment, as evidenced by deficits in adhesion and/or spreading, formation of long pseudopods, directional persistence of movement, and proliferative capacity. The observed requirement for ILK in responses to ECM proteins in melanocytes suggests that ILK also may coordinate melanoblast interactions with their surrounding environment through collagen and laminin receptors. ILK is a central component of various signaling modules that contribute to cell migration, including integrins, Rac1, and both the microtubule and F-actin networks (Jackson et al., 2015; Li et al., 2011; Nakrieko et al., 2008; Sayedyahossein et al., 2012). Both ILK and Rac1 modulate the frequency of formation of long pseudopodia in melanoblasts, which in turn contributes to their ability to move among adjacent cells in the developing embryo (Li et al., 2011). Thus, ILK might be an upstream modulator of Rac1 activation in embryonic melanoblasts.

Dendrites are morphologic hallmarks of melanocytic lineage cells and fulfill important functions as conduits for melanosome transfer to neighboring keratinocytes. Dendrite formation is a complex process triggered by activation of multiple signaling pathways in response to distinct agents, including peptide hormones, growth factors, and ECM proteins (Scott, 2002). We found that ILK^{KO} melanocytes have deficits in dendrite formation, and that bypassing Rac1 activation steps through exogenous expression of constitutively active Rac1 restored the ability of ILK^{KO} melanocytes to develop cell extensions in the presence of collagen. This is consistent with the proposal that collagen interactions with integrins likely trigger signaling pathways transmitted through ILK, which culminate in activation of Rac1 and induction of morphologic changes characterized by dendrite outgrowth.

In humans, benign nevus melanocytes can migrate from the skin to lymph nodes (Leblebici et al., 2016). Further, the highly metastatic behavior of melanomas has been ascribed, in these cells, to the expression of genes that participate in neural crest and melanoblast migration during embryonic development (Gupta et al., 2005; Lindsay et al., 2011). Similar to their embryonic precursors, interactions of melanoma cells with their surrounding environment lead to the activation of pronounced motile and invasive behavior. ILK expression is significantly increased in melanomas, relative to nevus melanocytes. ILK has also been implicated in mediating integrin β1-driven melanoma invasion and metastasis (El Kharbili et al., 2017). Thus, the identification of ILK as a key regulator of melanoblast motility may have potential important implications as a therapeutic target in human pathologies associated with melanocytic cell movements.

MATERIALS AND METHODS

Isolation and culture of mouse cutaneous melanoblasts and melanocytes

All animal experiments were approved by the University of Western Ontario Animal Care Committee (Protocol numbers 2016-022 and 2015-021), as per regulations and guidelines from the Canadian Council on Animal Care. Melanoblasts were isolated as previously described (Colombo et al., 2012), with some modifications. Skin was harvested from E15.5 mouse embryos, minced, and trypsinized. Single-cell suspensions were used for subsequent flow cytometry analysis or FACS. After FACS-purification, melanoblasts were seeded onto ST2 feeder layers for subsequent experiments. Mouse epidermal melanocytes were isolated from 3-day-old mice, cultured,

and transfected as described (Crawford et al., 2017; Dagnino and Crawford, 2019).

Microscopy

For indirect immunofluorescence microscopy analyses, melanocytes were processed as described elsewhere (Ivanova and Dagnino, 2007; Sayedyahossein et al., 2015). For melanocyte motility measurements, time-lapse videomicroscopy images were obtained during 16-hour intervals, and at least 20 cells per condition were tracked per experiment.

A detailed Materials and Methods section is available in the Supplementary Materials.

Data availability statement

No datasets were generated as part of these studies.

ORCIDs

Melissa Crawford: https://orcid.org/0000-0001-5559-2195
Valerie Leclerc: https://orcid.org/0000-0003-2442-4230
Kevin Barr: https://orcid.org/0000-0002-1550-0425
Lina Dagnino: https://orcid.org/0000-0003-1483-5159

CONFLICT OF INTEREST

The authors state no conflict of interest.

ACKNOWLEDGMENTS

MC and LD were supported by an Internal Grant from the Lawson Health Research Institute (F0588), by a "Quality of Life Trainee Support" grant from the Children's Health Research Institute and the Children's Health Foundation, and by an Ontario Graduate Scholarship. VL was supported by a "Dean's Undergraduate Research Opportunities Program" studentship from the Schulich School of Medicine and Dentistry (The University of Western Ontario). This work was supported by grants to LD from the Canadian Institutes of Health Research (FRN 110303) and the Natural Sciences and Engineering Research Council of Canada (RGPIN-2017-04765).

We thank K. Chadwick for expert help with flow cytometry and FACS, and I. Ivanova for comments on the manuscript.

AUTHOR CONTRIBUTIONS

Conceptualization: MC, LD; Formal Analysis: MC, LD; Funding Acquisition: LD; Investigation: MC, CL, KB, LD; Methodology: MC, LD; Project Administration: LD; Resources: LD; Supervision: LD; Validation: MC, LD; Visualization: MC, LD; Writing - Original Draft Preparation: MC; Writing - Review and Editing: LD.

SUPPLEMENTARY MATERIAL

Supplementary material is linked to the online version of the paper at www.jidonline.org, and at https://doi.org/10.1016/j.jid.2019.07.681.

REFERENCES

Adameyko I, Lallemend F, Aquino JB, Pereira JA, Topilko P, Müller T, et al. Schwann cell precursors from nerve innervation are a cellular origin of melanocytes in skin. Cell 2009;139:366–79.

Baxter LL, Pavan WJ. Pmel17 expression is Mitf-dependent and reveals cranial melanoblast migration during murine development. Gene Expr Patterns 2003;3:703–7.

Colombo S, Champeval D, Rambow F, Larue L. Transcriptomic analysis of mouse embryonic skin cells reveals previously unreported genes expressed in melanoblasts. J Invest Dermatol 2012;132:170–8.

Crawford M, Leclerc V, Dagnino L. A reporter mouse model for in vivo tracing and in vitro molecular studies of melanocytic lineage cells and their diseases. Biol Open 2017;6:1219–28.

Dagnino L, Crawford M. Isolation, culture, and motility measurements of epidermal melanocytes from GFP-expressing reporter mice. Methods Mol Biol 2019;1879:243–56.

Dai X, Jiang W, Zhang Q, Xu L, Geng P, Zhuang S, et al. Requirement for integrin-linked kinase in neural crest migration and differentiation and outflow tract morphogenesis. BMC Biol 2013;11:107.

Delmas V, Beermann F, Martinozzi S, Carreira S, Ackermann J, Kumasaka M, et al. Beta-catenin induces immortalization of melanocytes by suppressing p16INK4a expression and cooperates with N-Ras in melanoma development. Genes Dev 2007;21:2923–35.

El Kharbili M, Robert C, Witkowski T, Danty-Berger E, Barbollat-Boutrand L, Masse I, et al. Tetraspanin 8 is a novel regulator of ILK-driven beta 1 integrin adhesion and signaling in invasive melanoma cells. Oncotarget 2017;8:17140–55.

Gupta PB, Kuperwasser C, Brunet JP, Ramaswamy S, Kuo WL, Gray JW, et al. The melanocyte differentiation program predisposes to metastasis after neoplastic transformation. Nat Genet 2005;37:1047–54.

Haass NK, Smalley KS, Li L, Herlyn M. Adhesion, migration and communication in melanocytes and melanoma. Pigment Cell Res 2005;18:150–9.

Hara M, Yaar M, Tang A, Eller MS, Reenstra W, Gilchrest BA. Role of integrins in melanocyte attachment and dendricity. J Cell Sci 1994;107:2739–48.

Ho E, Dagnino L. Epidermal growth factor induction of front-rear polarity and migration in keratinocytes is mediated by integrin-linked kinase and ELMO2. Mol Biol Cell 2012;23:492–502.

Im M, Dagnino L. Protective role of integrin-linked kinase against oxidative stress and in maintenance of genomic integrity. Oncotarget 2018;9:13637–51.

Ivanova IA, Dagnino L. Activation of p38- and CRM1-dependent nuclear export promotes E2F1 degradation during keratinocyte differentiation. Oncogene 2007;26:1147–54.

Jackson BC, Ivanova IA, Dagnino L. An ELMO2-RhoG-ILK network modulates microtubule dynamics. Mol Biol Cell 2015;26:2712–25.

Laurent-Gengoux P, Petit V, Aktary Z, Gallagher S, Tweedy L, Machesky L, et al. Simulation of melanoblast displacements reveals new features of developmental migration. Development 2018;145:dev160200.

Le Douarin NM, Dupin E. The "beginnings" of the neural crest. Dev Biol 2018;444:S3–13.

Leblebici C, Kelten C, Gurel MS, Hachasasanoglu E. Intralymphatic nevus cells in benign nevi. Ann Diagn Pathol 2016;25:1–6.

Li A, Ma Y, Yu X, Mort RL, Lindsay CR, Stevenson D, et al. Rac1 drives melanoblast organization during mouse development by orchestrating pseudopod- driven motility and cell-cycle progression. Dev Cell 2011;21:722–34.

Lindsay CR, Lawn S, Campbell AD, Faller WJ, Rambow F, Mort RL, et al. P-Rex1 is required for efficient melanoblast migration and melanoma metastasis. Nat Commun 2011;2:555.

Lorenz K, Grashoff C, Torka R, Sakai T, Langbein L, Bloch W, et al. Integrin-linked kinase is required for epidermal and hair follicle morphogenesis. J Cell Biol 2007;177:501–13.

Luciani F, Champeval D, Herbette A, Denat L, Aylaj B, Martinozzi S, et al. Biological and mathematical modeling of melanocyte development. Development 2011;138:3943–54.

Moore R, Larue L. Cell surface molecules and truncal neural crest ontogeny: a perspective. Birth Defects Res C Embryo Today 2004;72:140–50.

Mort RL, Jackson IJ, Patton EE. The melanocyte lineage in development and disease. Development 2015;142:620–32.

Mould AP, Askari JA, Barton S, Kline AD, McEwan PA, Craig SE, et al. Integrin activation involves a conformational change in the alpha 1 helix of the beta subunit A-domain. J Biol Chem 2002;277:19800–5.

Nakrieko KA, Welch I, Dupuis H, Bryce D, Pajak A, St Arnaud R, et al. Impaired hair follicle morphogenesis and polarized keratinocyte movement upon conditional inactivation of integrin-linked kinase in the epidermis. Mol Biol Cell 2008;19:1462–73.

Petit V, Larue L. Any route for melanoblasts to colonize the skin! Exp Dermatol 2016;25:669–73.

Robinson CL, Evans RD, Sivarasa K, Ramalho JS, Briggs DA, Hume AN. The adaptor protein melanophilin regulates dynamic myosin-Va:cargo interaction and dendrite development in melanocytes. Mol Biol Cell 2019;30:742–52.

Sakai T, Li S, Docheva D, Grashoff C, Sakai K, Kostka G, et al. Integrin-linked kinase (ILK) is required for polarizing the epiblast, cell adhesion, and controlling actin accumulation. Genes Dev 2003;17:926–40.

Sayedyahossein S, Nini L, Irvine TS, Dagnino L. Essential role of integrin-linked kinase in regulation of phagocytosis in keratinocytes. FASEB J 2012;26:4218–29.

Sayedyahossein S, Rudkouskaya A, Leclerc V, Dagnino L. Integrin-linked kinase is indispensable for keratinocyte differentiation and epidermal barrier function. J Invest Dermatol 2016;136:425–35.

Sayedyahossein S, Xu SX, Rudkouskaya A, McGavin MJ, McCormick JK, Dagnino L. Staphylococcus aureus keratinocyte invasion is mediated by integrin-linked kinase and Rac1. FASEB J 2015;29:711–23.

Scott G. Rac and rho: the story behind melanocyte dendrite formation. Pigment Cell Res 2002;15:322–30.

Scott G, Leopardi S. The cAMP signaling pathway has opposing effects on Rac and Rho in B16F10 cells: implications for dendrite formation in melanocytic cells. Pigment Cell Res 2003;16:139–48.

Shi H, Lin B, Huang Y, Wu J, Zhang H, Lin C, et al. Basic fibroblast growth factor promotes melanocyte migration via activating PI3K/Akt-Rac1-FAK-JNK and ERK signaling pathways. IUBMB Life 2016;68:735–47.

Testaz S, Duband JL. Central role of the alpha4beta1 integrin in the coordination of avian truncal neural crest cell adhesion, migration, and survival. Dev Dyn 2001;222:127–40.

Tokuo H, Bhawan J, Coluccio LM. Myosin X is required for efficient melanoblast migration and melanoma initiation and metastasis. Sci Rep 2018;8:10449.

Vakaloglou KM, Chrysanthis G, Rapsomaniki MA, Lygerou Z, Zervas C. IPP complex reinforces adhesion by relaying tension-dependent signals to inhibit integrin turnover. Cell Rep 2016;14:2668–82.

Wang X, Astrof S. Neural crest cell-autonomous roles of fibronectin in cardiovascular development. Development 2016;143:88–100.

Watanabe N, Motohashi T, Nishioka M, Kawamura N, Hirobe T, Kunisada T. Multipotency of melanoblasts isolated from murine skin depends on the Notch signal. Dev Dyn 2016;245:460–71.

Woodham EF, Paul NR, Tyrrell B, Spence HJ, Swaminathan K, Scribner MR, et al. Coordination by Cdc42 of actin, contractility, and adhesion for melanoblast movement in mouse skin. Curr Biol 2017;27:624–37.

SUPPLEMENTARY MATERIALS AND METHODS

Mouse strains

All animal experiments were approved by the University of Western Ontario Animal Care Committee (Protocol numbers 2016-022 and 2015-021), as per regulations and guidelines from the Canadian Council on Animal Care. *Tyr::CreER^{T2}* mice, which express Cre-recombinase fused to a modified estrogen receptor under the control of the *Tyr* promoter (Bosenberg et al., 2006), were purchased from the Jackson Laboratory (*B6.Cg-Tg [Tyr-cre/ERT2]13Bos/J*, Stock 02328; Bar Harbor, ME). These animals were bred with mice homozygous for the *ROSA$^{mT/mG}$* reporter allele (Muzumdar et al., 2007) and the *Ilk^{tm1Star}* allele, in which the *Ilk* gene is flanked by loxP sites (Terpstra et al., 2003), which were a generous gift from Dr Rashmi Kothary (Ottawa Hospital Research Institute; Michalski et al., 2016). The mice used in the present studies were homozygous for the *Tyr::CreER^{T2}* and the *ROSA$^{mT/mG}$* alleles, and either homozygous (*Tyr::CreER^{T2}; ROSA$^{mT/mG}$; Ilk$^{f/f}$*, hereafter termed ILK^{KO}) or heterozygous (hereafter termed ILK^{+}) for the loxP-flanked *Ilk^{tm1Star}* allele. Genotyping was conducted as previously described (Sayedyahossein et al., 2015). The primer sequences used to genotype mouse strains were the following: *Cre* forward, 5′-CCATCTGCCACCAGCCAG-3′, and *Cre* reverse, 5′-TCGCCATCTTCCAGCAGG-3′ (amplicon size 281 base pairs [bp]); *Cpxm1* forward, 5′-TCGCCATCTTCCAGCAGG-3′, and *Cpxm1* reverse, 5′-GATGTTGGGGCACTGCTCATTCACC-3′ (amplicon size 420 bp). *Ilk* alleles were genotyped using two primer sets: *Ilk* forward, 5′-CTGTTGCAATACAAGGCTGAC-3′, and *Ilk* reverse, 5′-CTGGGAGAAGCTCTCTAAGGGG-3′ (amplicon size, 350 bp with wild type allele, and 384 bp with loxP-containing allele). The second set of primers has been described (Terpstra et al., 2003), and yields a 1.9-kb amplicon corresponding to the wild type allele, a 2.1-kb amplicon corresponding to the loxP-containing allele, and a 230-bp fragment corresponding to the Cre-excised *Ilk* allele. To induce Cre-recombinase–mediated gene excision, tamoxifen (1 mg per 25 g of body weight, dissolved in ethanol, Cremophor, phosphate buffered saline [PBS] 1:1:5 v/v) was administered intraperitoneally once to 11.5 days after coitus pregnant dams. Midday of the vaginal plug was considered as 0.5 days after coitus. In vivo tracing studies were conducted with at least five embryos harvested from three or more litters.

Cell lines, reagents, antibodies, and vectors

ST2 mouse bone marrow–derived mesenchymal cells (cell number RCB 0224; Ogawa et al., 1988) were purchased from the Riken Research Institute Cell Bank (Wako, Saitama, Japan). These cells were maintained in RPMI 1640 medium supplemented with 10% fetal bovine serum.

Rat tail collagen type I (354236) was purchased from Corning (Corning, NY) and endothelin-3 (CC-4510) was purchased from Lonza (Walkersville, MD). (Z)-4-hydroxytamoxifen (ab141943) was purchased form Abcam (Cambridge, United Kingdom). Lipofectamine 3000 (L3000-001), 2.5% trypsin (R-001-100), trypsin neutralizer solution (R-002-100), and the Annexin V Apoptosis Detection Kit eFluor450 (88-8006) were purchased from Thermo Fisher (Carlsbad, CA). Immu-mount mounting medium (9990402) was purchased from Fisher Scientific (Ottawa, Ontario, Canada). Cremophor EL (also termed Kolliphor EL; C-5135), the In Vivo EdU Flow Cytometry Kit 647 (BCK-IV-FC-S), 7-aminoactinomycin D (7-AAD; catalog number A9400), and all other chemicals were purchased from Sigma Aldrich (St. Louis, MO). The following antibodies were purchased from Abcam: chicken anti-GFP (13970), rabbit anti-Ki67 (15580), and mouse anti-TYRP1 (3312). Mouse anti-ILK (611803) was purchased from BD Biosciences (Franklin Lakes, New Jersey). Rabbit anti-keratin 14 (PRB-155P) was purchased from Covance (Princeton, New Jersey). Mouse anti- glyceraldehyde-3-phosphate dehydrogenase (GAPDH; ADI-CSA-335-E) was purchased from Enzo Life Sciences (Brockville, Ontario, Canada). Mouse anti-V5 (MA5-15253) was purchased from Invitrogen/ThermoFisher, and Alexa Fluor-conjugated goat anti-mouse, goat anti-rabbit, and goat anti-chicken IgG were purchased from Molecular Probes/Invitrogen (Eugene, OR). The Caspase-Glo 3/7 Assay (G8090) was purchased from Promega (Madison, WI).

The recombinant adenovirus encoding green fluorescent protein (GFP) together with Cre-recombinase ("Ad-Cre-GFP", hereafter termed Ad-Cre, catalog number 1700) was purchased from Vector Biolabs (Philadelphia, PA). The plasmids encoding wild type and G12V mCardinal/V5-tagged human Rac1 were generated by PCR amplification, using as templates plasmids encoding the corresponding GFP-labeled human Rac1 proteins (Subauste et al., 2000). The resulting amplicons were cloned into the mCardinal-C1 plasmid (Chu et al., 2014), which was a gift from Michael Davidson and was obtained from Addgene (plasmid #54799; Watertown, MA). All plasmids were verified by dideoxy sequencing.

Isolation of cutaneous embryonic melanoblasts

Melanoblasts were isolated as previously described (Colombo et al., 2012), with some modifications. Skin was harvested from embryonic day 15.5 mouse embryos and minced. Each minced skin was digested by incubation in 0.5 ml of 2.5% trypsin for 10 minutes at 37 °C, with gentle rocking. Two volumes of trypsin neutralizer solution were added, followed by thorough mixing. The cell suspension generated was filtered through a 40 μm pore size strainer (431750, Corning, NY) to remove tissue debris and centrifuged (140*g* for 5 minutes at 22 °C). After removal of the supernatant, the cell pellet was suspended in PBS-containing 2% fetal bovine serum and transferred to 5-ml glass polystyrene tubes (352235; BD Biosciences, Franklin Lakes, New Jersey) for subsequent flow cytometry analysis or FACS.

Flow cytometry analysis and FACS of melanoblasts

Flow cytometry analysis was conducted on a Becton Dickinson FACS Canto Flow Cytometer (BD Biosciences, Mississauga, Ontario, Canada) with FACSDiVa software, version 8.0.1. The blue laser trigon was configured to detect GFP from detector B (530/30 bandpass and 502 long pass filter). The yellow-green laser octagon was configured to detect membrane-bound Tomato fluorescent protein (mTomato) from detector C (610/20 band pass and 600 long pass filter),

and 7-AAD from detector B (670/30 bandpass and 655 long pass filter). The following gating strategy was used to analyze viable GFP- and/or mTomato-positive cells. Viable cells were first selected based on exclusion of 7-AAD. Cell doublets were excluded based on consecutive gates on forward scatter—height versus forward scatter—width, and side scatter—height versus side scatter—width plots. GFP-positive cells were selected by comparison with GFP-negative control samples, which were composed of cells isolated from three different populations of melanoblasts as follows: cells isolated from *Tyr::CreER^{T2}*, *ROSA$^{mT/mG}$*, *Ilk$^{f/f}$*, and from *ROSA$^{m/TmG}$; Ilk$^{f/f}$* embryos not exposed to tamoxifen; and cells isolated from C57BL/6J embryos. The number of targeted GFP-expressing melanoblasts from each embryo was normalized to the total number of viable skin cells obtained (averaging approximately 5×10^5 cells per embryo).

For purification of targeted melanoblasts, embryonic skin cell suspensions were sorted using a Becton Dickinson FACSAria III cell sorter (BD Biosciences) with FACSDiVa software, version 8.0.1. To obtain >99% pure populations of viable targeted GFP-expressing melanoblasts, the blue laser trigon was configured to detect GFP from detector B (530/30 bandpass and 502 long pass filter). The yellow-green laser octagon was configured to detect mTomato from detector C (610/20 band pass and 600 long pass filter), and 7-AAD was detected from detector B (670/14 bandpass and 630 long pass filter). Embryonic skin cell suspensions were sorted at 4 °C, using a 100 m nozzle at low pressure (20 psi) and at a maximum event rate of 2000 events per second. Flow cytometry and FACS experiments were conducted at the London Regional Flow Cytometry Facility of the Robarts Research Institute.

Analysis of melanoblast proliferation and apoptosis

The fraction of apoptotic cells in embryonic melanoblast isolates was analyzed by flow cytometry, with eBioscience Annexin V Apoptosis Detection Kit eFluor 450 (88-8006; Thermo Fisher). Single-cell suspensions prepared from embryonic skin isolates were suspended in 1X Binding Buffer at a density of $1-3 \times 10^5$ cells per 100 µl, mixed with 10 µl of fluorochrome-conjugated Annexin V, and incubated for 15 minutes at 22 °C in the dark. Cells were centrifuged and resuspended in 300 µl 1X Binding Buffer. To stain non-viable cells, 5 µl of 7-AAD (50 µg/ml dissolved in PBS) were added to each sample. Targeted, GFP-positive melanoblasts were immediately analyzed on a Becton Dickinson FACS Canto Flow Cytometer as described above. In addition, the violet/red laser octagon was configured to detect Annexin V eFluor450 from detector D (450/50 bandpass). The proportion of targeted early apoptotic (GFP^+, Annexin V^+, 7-AAD^-), late apoptotic (GFP^+, Annexin V^+, 7-AAD^+), and necrotic cells (GFP^+, Annexin V^-, 7-AAD^+) was determined. Samples consisting of cultured primary epidermal keratinocytes exposed to 100 J/m^2 UVB light 24 hours before Annexin V processing were used as positive controls for apoptosis (Singh and Dagnino, 2016).

Melanoblast culture and motility measurements

ST2 cells were plated into the wells of four-well culture inserts included with 35 mm µ-dishes (80466, Ibidi, Madison, WI), at a density of 7, 000 cells per 0.03 cm^2 well, and cultured in ST2 growth medium for 24 hours. Pooled GFP-expressing melanoblasts from genotype-matched embryos were FACS-sorted and seeded onto the confluent ST2 monolayers in which the culture medium had been replaced with a mixture of 50 µl RPMI medium supplemented with 10% fetal bovine serum and 50 µl of melanocyte growth medium just before addition of embryonic melanoblasts. Sixteen hours later, the motility of GFP-positive cells was recorded during 3-hour periods by time-lapse videomicroscopy with a Leica DMIRBE fluorescence microscope equipped with an ORCA-ER digital camera (Hamamatsu Photonics, Hamamatsu City, Shizuoka, Japan), using Volocity 6.1.1 software (Improvision, Coventry, United Kingdom). The cells were manually tracked using the Manual Tracking Version-1 plugin for ImageJ software, version 1.50i (Fiji, NIH). The speed, accumulated distance, and directionality of each cell were calculated using MTrackJ and the ImageJ Chemotaxis & Migration Tool, version 1.48 (Ibidi). Ten to 20 cells were tracked in each individual experiment.

Melanocyte isolation, culture, and transfection

Mouse epidermal melanocytes were isolated from 3-day-old mice, cultured, and transfected with Lipofectamine 3000 (L3000-001; Thermo Fisher), as we previously described (Crawford et al., 2017; Dagnino and Crawford, 2019). All experiments were conducted with passage-2 or -3 cultures. Normal melanocyte growth medium consisted of MBM-4 basal medium (CC-4435; Lonza, Walkersville, MD) containing endothelin-3 (260 ng/ml, final) and growth supplements, including insulin, basic fibroblast growth factor, and bovine pituitary extract (CC-4435; Lonza). Where indicated, melanocytes were plated on laminin-332 matrix isolated from 804G rat bladder squamous carcinoma cell conditioned medium (Tripathi et al., 2008) or cultured for 24 hours in CnT-PR-MD medium ("MD medium") purchased from CellNTec (Stauffacherstrasse, Bern, Switzerland). To induce Cre-mediated recombination, melanocytes were cultured in medium containing 1 µM 4-hydroxytamoxifen or ethanol, as control vehicle, for 48 hours. After a PBS rinse, the cells were cultured in melanocyte growth medium for an additional 72-hour period, unless otherwise indicated. ILK-deficient melanocytes were identified through GFP epifluorescence. For adenoviral transduction, cells were cultured in the presence of Ad-Cre viruses diluted in melanocyte growth medium at a multiplicity of infection of 120. Four hours later, the medium was removed, melanocytes were rinsed once with PBS and cultured in melanocyte growth medium for 5 days. Under these conditions, transduction efficiency was ≥95%, with no significant loss of cell viability.

Immunohistochemistry, immunofluorescence, and time-lapse videomicroscopy

Paraffin-embedded 7 µm sections of embryonic skin were deparaffinized and subjected to high-temperature antigen retrieval with 10 mM sodium citrate (pH 6.0), followed by incubation with primary antibodies, as described elsewhere (Rudkouskaya et al., 2014; Sayedyahossein et al., 2016). For indirect immunofluorescence microscopy analyses, melanocytes were fixed in freshly diluted 4% paraformaldehyde and

processed as described elsewhere (Ivanova and Dagnino, 2007; Sayedyahossein et al., 2015). Fluorescence and phase-contrast micrographs of fixed specimens were obtained with a Leica DMIRBE fluorescence microscope equipped with an ORCA-ER digital camera (Hamamatsu Photonics), using Volocity 6.1.1 software (Improvision). For melanocyte motility measurements, cells were seeded in 35 mm μ-dishes (81156; Ibidi), and time-lapse videomicroscopy images were obtained during 16-hour intervals as described above for melanoblast motility assays. At least 20 cells per condition were tracked in each experiment. For experiments with Rac1-encoding plasmids, melanocytes were seeded in 24-well μ-dishes (82046; Ibidi) that had been coated with Collagen Type I (15 μg/cm^2). Melanocyte circularity values were calculated using the formula $4\pi A/P^2$, where A = cell surface area and P = cell perimeter (Robinson et al., 2019).

Immunoblot analysis

Cell lysates were prepared in a modified radioimmunoprecipitation assay (RIPA) buffer (50 mM Tris-HCl pH 7.4, 150 mM NaCl, 1% NP-40, 0.5% sodium deoxycholate, 0.1% SDS, 1 mM Na_3VO_4, 5 mM NaF, 1 mM phenylmethylsulfonyl fluoride, 10 mg/ml each aprotinin, leupeptin, and pepstatin). Proteins in lysates were resolved by denaturing polyacrylamide gel electrophoresis and transferred to polyvinyledene fluoride membranes, which were probed with antibodies against proteins indicated in individual experiments.

Caspase-3/7 activity measurements

Melanocytes were seeded in 96-well plates at a density of 15×10^3 melanocytes per well and cultured for 24 hours. Caspase-3/7 activity was measured using Caspase-Glo Assay kits, according to the manufacturer's instructions. The Caspase-Glo Reagent was prepared by thoroughly mixing the reaction buffer and the substrate supplied in the kit, prewarmed to 22 °C. The reagent was added to the cells (100 μl/well), followed by incubation at 22 °C for 2 hours. Caspase-3/7 activity-associated luminescence was then measured in triplicate samples, using a Wallac Victor3 V plate reader (Perkin Elmer, Waltham, MA).

Analysis of cell spreading and dendrite outgrowth after treatment with Mn^{2+}

After treatment with ethanol or 4-hydroxytamoxifen, melanocytes were trypsinized and resuspended in MBM-4 basal medium without endothelin-3 or growth supplements, but containing 0.1 mM $MnCl_2$. The cells were seeded onto four-well culture dishes (uncoated, coated with laminin 332 matrix, or with 15 μg/cm^2 collagen I), at a density of 12, 500 cells per cm^2 well. Cell morphology was analyzed from mTomato or mGFP fluorescence micrographs, using ImageJ software, version 1.50i (Fiji, NIH). Changes in melanocyte circularity, used as a measure of dendrite outgrowth, were assessed 30 and 60 minutes after plating on uncoated or laminin 332-coated surfaces. For melanocytes seeded on collagen I, cell surface area was measured 2 hours after plating, by manually rendering the cell contour in the mTomato or mGFP fluorescence micrographs. Sixty cells per treatment were scored from three independent cell isolates.

Quantification of active Rac1 levels

Rac1-GTP abundance was measured using a luminescence-based G-LISA Rac1 activation kit (BK126; Cytoskeleton, Denver, CO), according to the manufacturer's instructions. For these experiments, melanocytes were cultured in growth medium containing 1 μM 4-hydroxytamoxifen or ethanol for 48 hours to induce Cre-mediated *Ilk* excision. The cells were then trypsinized, seeded onto 60 mm uncoated culture dishes (300,000 cells per dish), and cultured in normal melanocyte growth medium for an additional 48-hour period. After removal of the growth medium and two PBS rinses, melanocytes were cultured for 16 hours in MBM-4 basal medium without endothelin-3 or growth supplements. To activate Rac1, the MBM-4 basal medium was replaced with prewarmed complete growth medium containing endothelin-3 and growth supplements. The cells were incubated at 37 °C and lysates were prepared at timed intervals thereafter, using the lysis buffer supplied with the G-LISA Rac1 activation kit. Rac1-GTP-associated luminescence was measured at 440 nm in a Wallac Victor3 plate reader (Perkin Elmer, Waltham, MA), using duplicate lysate samples containing 1 μg protein each. In each experiment, background luminescence was measured in protein-free lysis buffer and was subtracted from values obtained with cell lysates.

Statistical analysis

Data were analyzed, as appropriate, using Student *t* test, and one- or two-way analysis of variance with post hoc Tukey's correction, using Prism 6 software, version 6.0c. Significance was set at $P < 0.05$. Experiments with cultured melanocytes were conducted in duplicate or triplicate samples at least three times, and using independent cell isolates.

SUPPLEMENTARY REFERENCES

Bosenberg M, Muthusamy V, Curley DP, Wang Z, Hobbs C, Nelson B, et al. Characterization of melanocyte-specific inducible Cre-recombinase transgenic mice. Genesis 2006;44:262–7.

Chu J, Haynes RD, Corbel SY, Li P, González-González E, Burg JS, et al. Non-invasive intravital imaging of cellular differentiation with a bright red-excitable fluorescent protein. Nat Methods 2014;11:572–8.

Colombo S, Champeval D, Rambow F, Larue L. Transcriptomic analysis of mouse embryonic skin cells reveals previously unreported genes expressed in melanoblasts. J Invest Dermatol 2012;132:170–8.

Crawford M, Leclerc V, Dagnino L. A reporter mouse model for in vivo tracing and in vitro molecular studies of melanocytic lineage cells and their diseases. Biol Open 2017;6:1219–28.

Dagnino L, Crawford M. Isolation, culture, and motility measurements of epidermal melanocytes from GFP-expressing reporter mice. Methods mol biol 2018.

Ivanova IA, Dagnino L. Activation of p38- and CRM1-dependent nuclear export promotes E2F1 degradation during keratinocyte differentiation. Oncogene 2007;26:1147–54.

Michalski JP, Cummings SE, O'Meara RW, Kothary R. Integrin-linked kinase regulates oligodendrocyte cytoskeleton, growth cone, and adhesion dynamics. J Neurochem 2016;136:536–49.

Muzumdar MD, Tasic B, Miyamichi K, Li L, Luo L. A global double-fluorescent Cre reporter mouse. Genesis 2007;45:593–605.

Ogawa M, Nishikawa S, Ikuta K, Yamamura F, Naito M, Takahashi K, et al. B cell ontogeny in murine embryo studied by a culture system with the monolayer of a stromal cell clone, ST2: B cell progenitor develops first in the embryonal body rather than in the yolk sac. EMBO J 1988;7:1337–43.

Robinson CL, Evans RD, Sivarasa K, Ramalho JS, Briggs DA, Hume AN. The adaptor protein melanophilin regulates dynamic myosin-Va:cargo interaction and dendrite development in melanocytes. Mol Biol Cell 2019;30:742–52.

Rudkouskaya A, Welch I, Dagnino L. ILK modulates epithelial polarity and matrix formation in hair follicles. Mol Biol Cell 2014;25:620–32.

Sayedyahossein S, Rudkouskaya A, Leclerc V, Dagnino L. Integrin-linked kinase is indispensable for keratinocyte differentiation and epidermal barrier function. J Invest Dermatol 2016;136:425–35.

Sayedyahossein S, Xu SX, Rudkouskaya A, McGavin MJ, McCormick JK, Dagnino L. Staphylococcus aureus keratinocyte invasion is mediated by integrin-linked kinase and Rac1. FASEB J 2015;29:711–23.

Singh RK, Dagnino L. E2F1 interactions with hHR23A inhibit its degradation and promote DNA repair. Oncotarget 2016;7:26275–92.

Subauste MC, Von Herrath M, Benard V, Chamberlain CE, Chuang TH, Chu K, et al. Rho family proteins modulate rapid apoptosis induced by cytotoxic T lymphocytes and Fas. J Biol Chem 2000;275:9725–33.

Terpstra L, Prud'homme J, Arabian A, Takeda S, Karsenty G, Dedhar S, et al. Reduced chondrocyte proliferation and chondrodysplasia in mice lacking the integrin-linked kinase in chondrocytes. J Cell Biol 2003;162:139–48.

Tripathi M, Nandana S, Yamashita H, Ganesan R, Kirchhofer D, Quaranta V. Laminin-332 is a substrate for hepsin, a protease associated with prostate cancer progression. J Biol Chem 2008;283:30576–84.

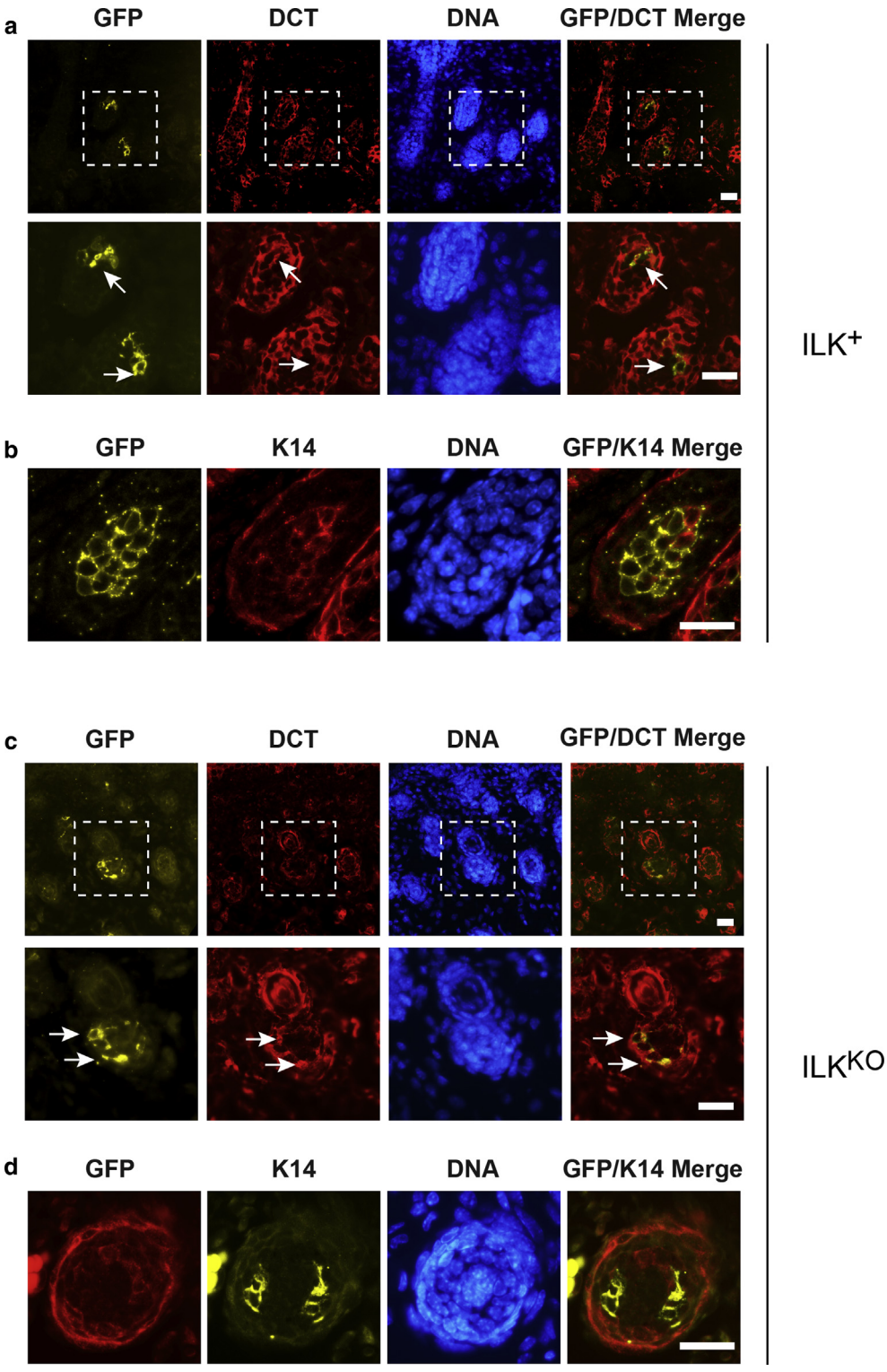

Supplementary Figure S1. Tamoxifen-mediated Cre targeting of first wave melanocytic lineage cells in vivo. Skin sections showing hair follicles from E20.5 ILK^{+} or ILK^{KO} littermate embryos isolated from a dam treated with tamoxifen at 11.5 days of gestation were processed for IF microscopy. (**a, c**) Sections were immunostained using antibodies against GFP or DCT. (**b, d**) Sections were immunostained using antibodies against GFP or K14. DNA was visualized with Hoescht 33342. Insets in panels a and c are shown at higher magnification in the accompanying micrographs directly underneath. Arrows indicate the position of representative GFP-expressing DCT-positive cells. DCT, dopachrome-tautomerase; E, embryonic day; GFP, green fluorescent protein; IF, immunofluorescence; ILK, integrin-linked kinase; K14, keratin 14; KO, knockout. Bars = 25 μm.

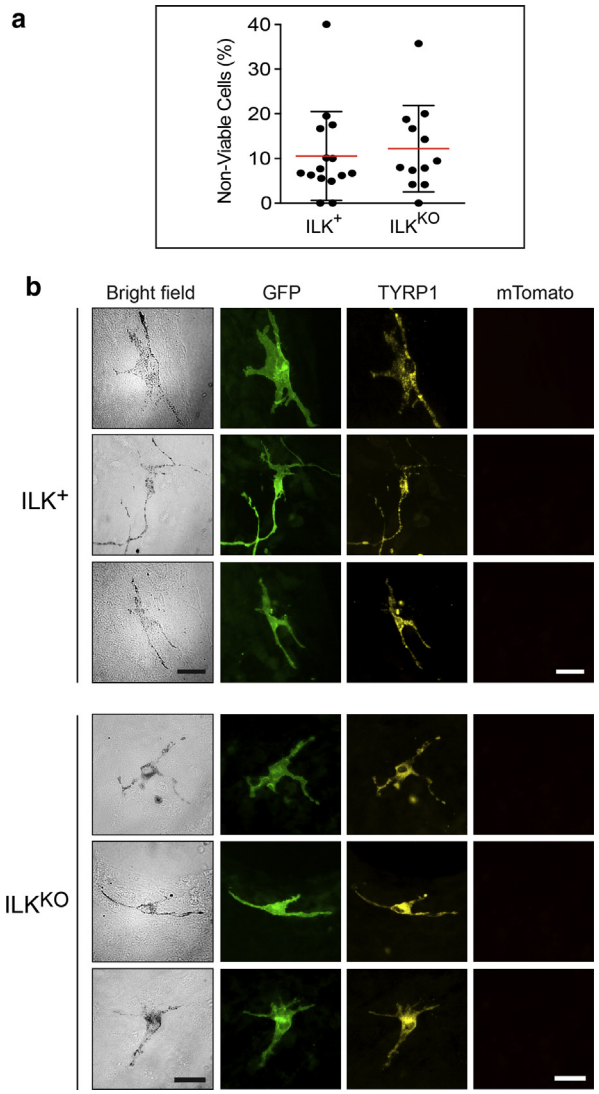

Supplementary Figure S2. Differentiation of melanoblasts into melanin-producing cells in culture. (**a**) Single-cell suspensions were obtained from the skin of E15.5 ILK^{+} and ILK^{KO} embryos exposed to tamoxifen at E11.5. The cells were analyzed by flow cytometry to determine the fraction of GFP-positive non-viable melanoblasts that exhibited 7-AAD and/or Annexin V fluorescence. The data are plotted as the percentage of non-viable GFP-expressing cells in individual tamoxifen-treated embryos obtained from 4–5 independent litters of ILK^{+} and ILK^{KO} mice. The lines in the graph represent the mean and SD of GFP-positive non-viable cells for each genotype. (**b**) FACS-purified GFP-positive melanoblasts isolated from E15.5 tamoxifen-treated embryos were cultured on ST2 feeder layers for 7 days and processed for IF microscopy using antibodies against GFP or TYRP1. The specimens were also examined for mTomato direct fluorescence. Bright-field images with pigment-containing cells are shown on the left.7-AAD, 7-Aminoactinomycin D; E, embryonic day; GFP, green fluorescent protein; IF, immunofluorescence; ILK, integrin-linked kinase; KO, knockout; mTomato, membrane-bound Tomato fluorescent protein; SD, standard deviation. Bar = 25 μm.

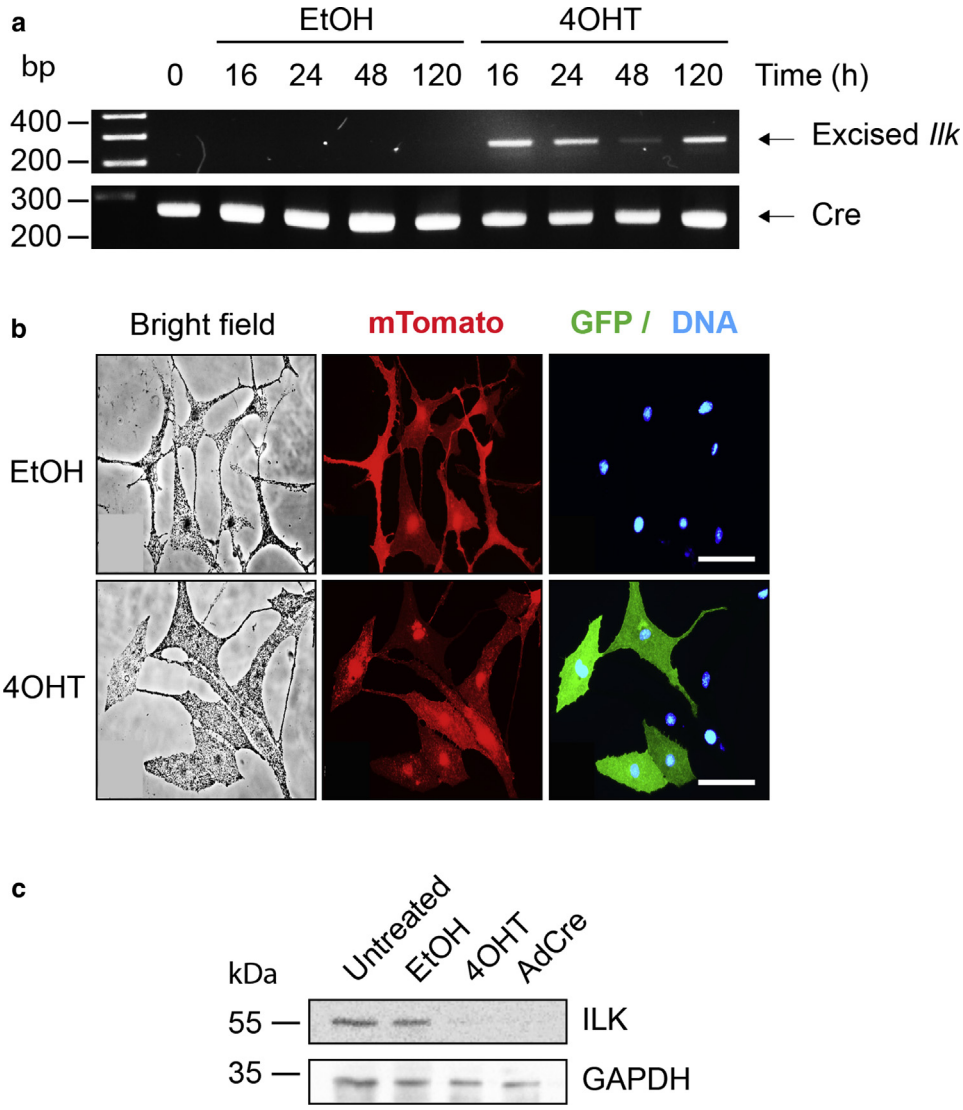

Supplementary Figure S3. Inactivation of *Ilk* in cultured postnatal melanocytes. Epidermal melanocytes were isolated from 3-day-old *TyrCreERT2, mT/mG, Ilk*$^{f/f}$ mice and cultured to passage 2–3. (**a**) Cells were treated with 1 μM 4-OHT or control vehicle (0.25% EtOH) for 48 hours. Genomic DNA was isolated at the indicated times after the initial addition of 4-OHT or EtOH, and analyzed by PCR. Amplicons corresponding to the Cre-excised *Ilk* (230 bp) or the Cre allele (280 bp) are shown. (**b**) Melanocytes were treated with EtOH or 4-OHT as in panel a and processed for microscopy 120 hours later. Phase-contrast, mTomato direct fluorescence or GFP IF are shown. DNA was visualized with Hoechst 333412. **(c)** Melanocytes were treated with EtOH or 4-OHT as in panel a, or transduced for 4 hours with a Cre-encoding adenovirus at a MOI of 120. After 5 days in culture, GFP^{+} cells in 4-OHT-treated samples were FACS-purified, and cell lysates from each treatment group were prepared and analyzed by immunoblot with antibodies against ILK or GAPDH (used as loading control). bp, base pairs; EtOH, ethanol; GAPDH, glyceraldehyde-3-phosphate dehydrogenase; GFP, green fluorescent protein; IF, immunofluorescence; ILK, integrin-linked kinase; MOI, multiplicity of infection; mTomato, membrane-bound Tomato fluorescent protein; 4-OHT, 4-hydroxytamoxifen. Bar = 64 μm.

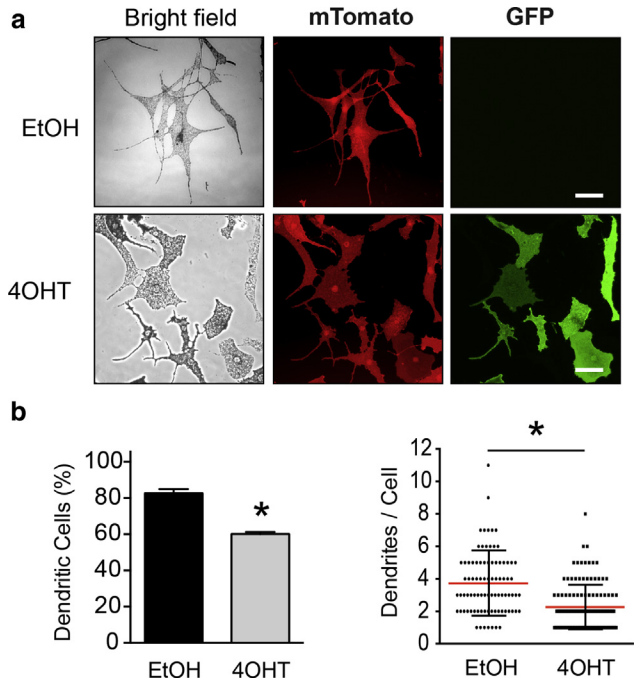

Supplementary Figure S4. Impaired dendrite formation in ILK-deficient melanocytes in response to laminin-332. Epidermal melanocytes were isolated from 3-day-old *TyrCreERT2, mT/mG, Ilk*$^{f/f}$ mice and cultured to passage 2−3. Cells were seeded on plates coated with laminin-332 substrate, and treated 1 day later with 1 μM 4-OHT or control vehicle (0.25% EtOH) for 48 hours. Five days after initial addition of 4-OHT, the cells were processed for microscopy. (**a**) Phase-contrast and fluorescence micrographs of melanocyte cultures. mTomato and GFP were visualized by direct fluorescence or by IF, respectively, using anti-GFP antibodies. (**b**) The percentage of cells with at least one dendrite >14 μm in length and the number of dendrites per cell exclusively in dendrite-positive cells were determined, and are presented as the mean ± SEM. Only GFP-expressing cells were scored in the 4-OHT-treated cultures. *$P < 0.05$, Student *t* test (300 cells scored from three independent isolates). EtOH, ethanol; GFP, green fluorescent protein; IF, immunofluorescence; ILK, integrin-linked kinase; mTomato, membrane-bound Tomato fluorescent protein; 4-OHT, 4-hydroxytamoxifen; SEM, standard error of the mean. Bar = 50 μm.

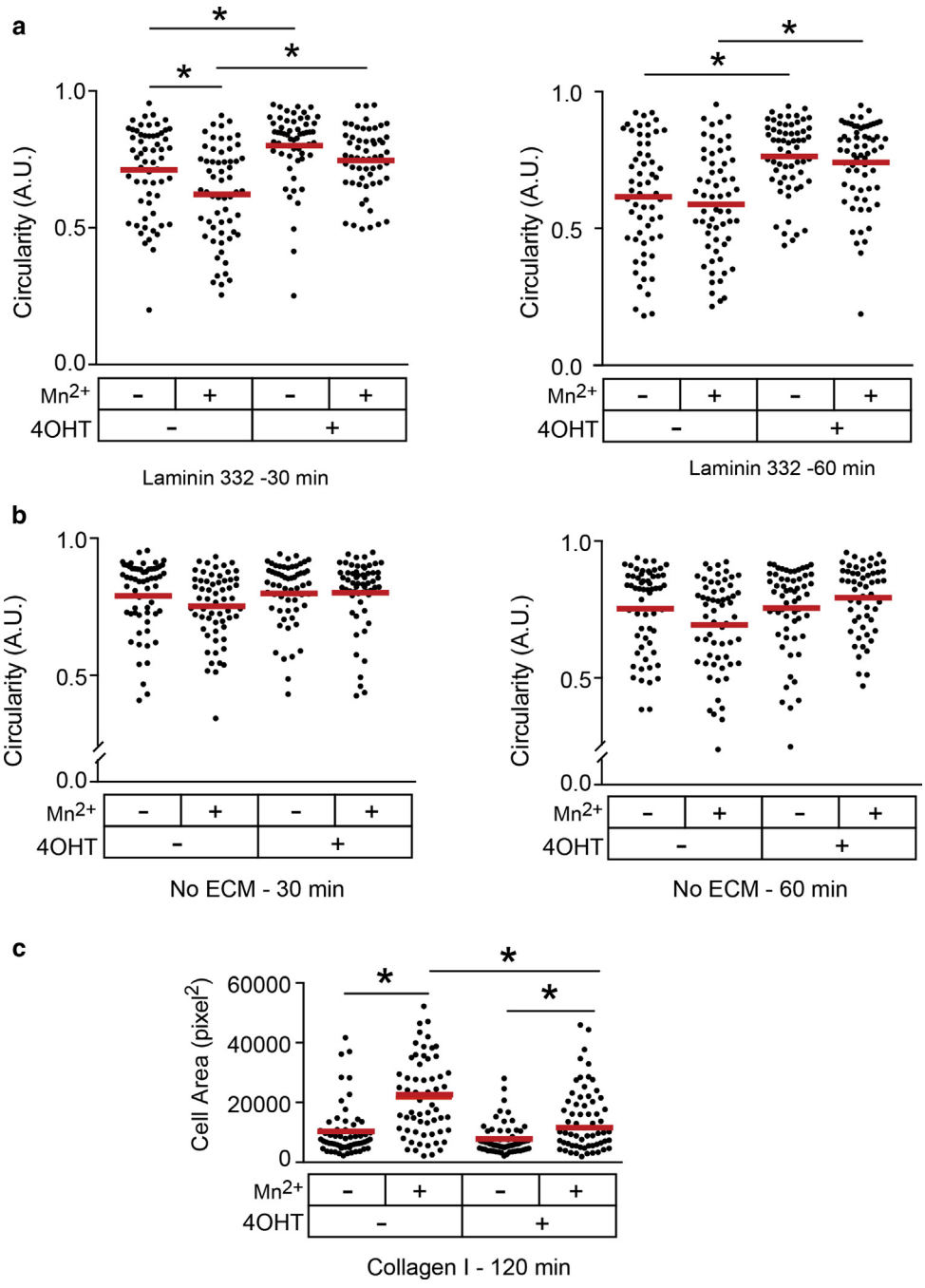

Supplementary Figure S5. Impaired responses to Mn^2 in ILK-deficient melanocytes. Epidermal melanocytes were treated with 1 μM 4-OHT or control vehicle (0.25% EtOH) for 48 hours, and cultured for an additional 72-hour interval. The cells were trypsinized and resuspended in MBM-4 basal medium without growth supplements, in the presence or absence of 0.1 mM $MnCl_2$. The cells were seeded on culture dishes coated with (**a**) laminin 332 matrix, (**b**) no exogenous matrix, or (**c**) 15 μg/cm^2 collagen I. At the indicated times after plating, circularity or surface area values were determined. The red lines in the dot plots represent the mean values for each treatment group. Only GFP^+ cells were scored in the 4-OHT-treated population. $^*P < 0.05$, ANOVA (60 cells per group from three independent isolates were scored). ANOVA, analysis of variance; EtOH, ethanol; GFP, green fluorescent protein; ILK, integrin-linked kinase; 4-OHT, 4-hydroxytamoxifen.

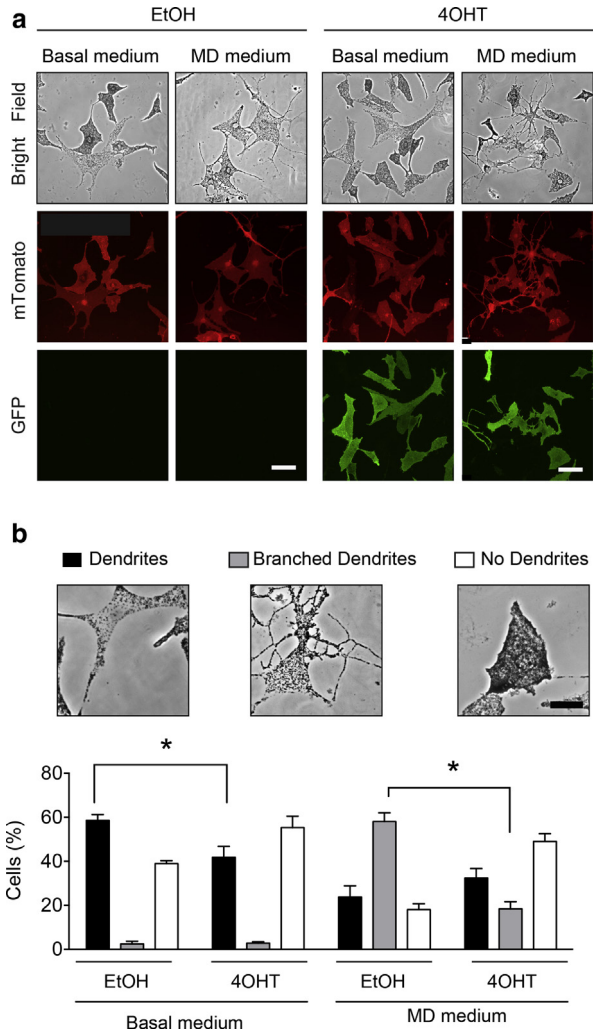

Supplementary Figure S6. Impaired dendrite formation in ILK-deficient melanocytes in response to soluble dendrite-inducing factors. Epidermal melanocytes were isolated from 3-day-old *TyrCreERT2, mT/mG, Ilk*$^{f/f}$ mice and cultured to passage 2−3. Cells were incubated with 1 μM 4-OHT or control vehicle (0.25% EtOH) for 48 hours. Four days after the initial addition of 4-OHT, the cells were cultured in normal growth medium ("Basal medium"), or medium supplemented with dendrite-inducing soluble factors ("MD medium") for 24 hours. The cells were then processed for microscopy. (a) Phase-contrast and fluorescence micrographs of melanocyte cultures in which mTomato and GFP were visualized, respectively, by direct fluorescence or by IF using anti-GFP antibodies. (b) The percentage of cells with at least one dendrite >14 μm in length ("Dendrites", black bars), with branched dendrites (gray bars), or without visible dendrites ("No dendrites", white bars) are shown as the mean ± SEM. Only GFP-expressing cells were scored in the 4-OHT-treated cultures. *$P < 0.05$, Student *t* test (300 cells scored from three independent isolates). EtOH, ethanol; GFP, green fluorescent protein; IF, immunofluorescence; ILK, integrin-linked kinase; mTomato, membrane-bound Tomato fluorescent protein; 4-OHT, 4-hydroxytamoxifen; SEM, standard error of the mean. Bar = 80 μm.

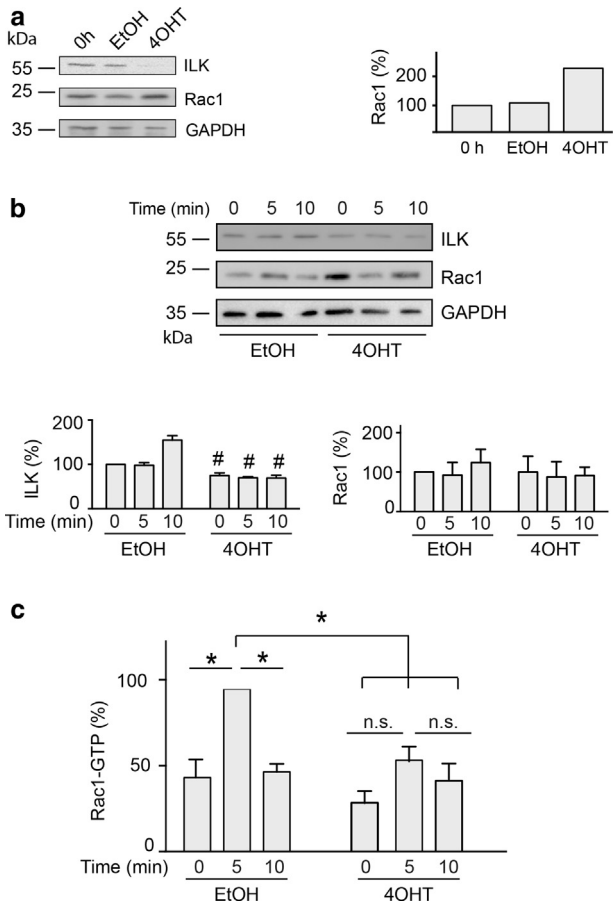

Supplementary Figure S7. Abnormal Rac1 activation in ILK-deficient melanocytes. (**a**) The immunoblots generated with lysates prepared from FACS-purified GFP^{+} cells in 4-OHT-treated samples shown in Supplementary Figure S3c were analyzed with anti-Rac1 antibodies. Rac1 intensity signals normalized to GAPDH are shown in the accompanying histogram, and are expressed relative to values in lysates from untreated cells. (**b**) Melanocytes were treated with EtOH or 1 μM 4-OHT for 48 hours, trypsinized, and cultured on uncoated dishes for 48 hours in normal growth medium. After incubation for 16 hours in growth supplement-free basal medium, the cells were stimulated with medium containing growth supplements, and lysed at the indicated times thereafter. A representative immunoblot probed with antibodies against ILK, Rac1, or GAPDH (used as a loading control) is shown. The histograms represent ILK or Rac1 abundance normalized to GAPDH, and are expressed as the mean ± SD relative to lysates from EtOH-treated melanocytes at t = 0, which are set to 100%. $^{\#}P < 0.05$, ANOVA (n = 3). **(c)** Rac1-GTP levels in the melanocyte lysates described in b were measured as detailed in the Supplementary Materials and Methods, and are expressed as the mean ± SD, relative to the maximum Rac1-GTP levels measured, which are set to 100%. *$P < 0.005$, ANOVA (n = 3). ANOVA, analysis of variance; EtOH, ethanol; GAPDH, glyceraldehyde-3-phosphate dehydrogenase; GFP, green fluorescent protein; ILK, integrin-linked kinase; n.s., not significant; 4-OHT, 4-hydroxytamoxifen; SD, standard deviation.